AFFDL-TR-71-125

FABRICATION AND INSTRUMENTATION OF AN EXPERIMENTAL PASSIVE RADIATIVE INFRARED DETECTOR COOLER FOR SPACECRAFT APPLICATIONS

W. F. SCHMIDT

H. L. HILLESLAND

C. A. ZIERMAN

PHILCO-FORD CORPORATION

*** Export controls have been removed ***

TECHNICAL REPORT AFFDL-TR-71-125

OCTOBER 1971

AIR FORCE FLIGHT DYNAMICS LABORATORY
AIR FORCE SYSTEMS COMMAND
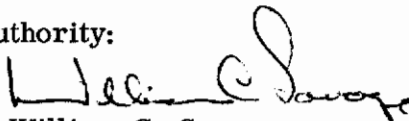WRIGHT-PATTERSON AIR FORCE BASE, OHIO 45433

FOREWORD

This report was prepared by the Western Development Laboratories Division of Philco-Ford Corporation under contract number F33615-71-C-1025. The work was administered under the direction of the Air Force Flight Dynamics Laboratory, Wright-Patterson Air Force Base with Mr. C. J. Feldmanis, AFFDL/FEE, acting as project engineer.

The report covers work conducted from 15 October 1970 to 15 October 1971.

This technical report has been reviewed and is approved.

Approving Authority:

William C. Savage
Environmental Control Branch
Vehicle Equipment Division
Air Force Flight Dynamics Laboratory

ABSTRACT

AFFDL-TR-71-125

A thermal experimental model of a passive radiative cooler for use on an earth orbiting spacecraft was fabricated, assembled, and tested in a thermal vacuum environment. The design of the cooler was based on the results of a previous thermal analysis and design study, performed by Philco-Ford for the Air Force Flight Dynamics Laboratory, Wright-Patterson Air Force Base.

The cooler was assumed to be used on a spacecraft in a 200 nautical mile altitude earth orbit in the plane of the ecliptic. The objective of the program was to verify the thermal performance of the cooler. Thermal analysis predicted an orbital temperature of 146° R for the radiator of the cooler. The tests produced higher than predicted temperatures for the radiator. Depending on the test conditions, a temperature of 246°R to 200°R was achieved for

- -

the radiator. The primary reasons for the higher than predicted temperatures were identified as higher than predicted thermal conductances between the simulated spacecraft and the cooler shield and radiator surfaces.

This document is subject to special export controls and each transmittal to foreign governments or foreign nationals may be made only with prior approval of AFFDL (FEE), Wright-Patterson Air Force Base, Ohio 45433.

THIS UNCLASSIFIED ABSTRACT IS DESIGNED FOR RETENTION IN A STANDARD 3–BY–5 CARD–SIZE FILE, IF DESIRED. WHERE THE ABSTRACT COVERS MORE THAN ONE SIDE OF THE CARD, THE ENTIRE RECTANGLE MAY BE CUT OUT AND FOLDED AT THE DOTTED CENTER LINE. (IF THE ABSTRACT IS CLASSIFIED, HOWEVER, IT MUST NOT BE REMOVED FROM THE DOCUMENT IN WHICH IT IS INCLUDED.)

WDL–2205 (1-63)

TABLE OF CONTENTS

LIST OF ILLUSTRATIONS

LIST OF ILLUSTRATIONS (Cont)

LIST OF TABLES

x

SECTION I

INTRODUCTION

The development and test of cryogenic temperature coolers is a key area of tech-
nology in the utilization of infrared detector systems for spacecraft applications.
All bodies emit energy as a function of their absolute temperature; this radiation
can be detected by infrared detectors with appropriate optics and electronics.
However, the signal-to-noise ratio and sensitivity of the detector is improved as
the detector temperature is decreased. Therefore, it is necessary to attain temper-
atures down to and below that of liquid nitrogen (140°R) to ensure proper per-
formance.

Due to their inherent simplicity and reliability, passive radiative coolers are
taking an increasingly important role in providing cryogenic temperatures for
infrared detectors. Expendable and closed cycle refrigerators have weight,
power, and reliability limitations for long lifetime missions.

In an earlier study performed by Philco-Ford for Wright-Patterson Air Force
Base under contract number F33615 - 69-C- 175 (reference 1), a feasibility and
development design study was performed on passive radiative detector coolers
for spacecraft applications. The intent of the study was to arrive at realistic
design concepts and tradeoff parameters. The spacecraft, carrying the detector
system, orbits the earth and is exposed to solar and planetary heat fluxes. The
radiative cooler rejects thermal energy to space and provides detector cooling
by thermal radiation. Based on the results of the feasibility study, the achieve-
ment of a radiator temperature of 140°R or lower is dependent on the orbital
parameters (including orbital altitude and orientation of the spacecraft with
respect to the earth and sun), shielding of the detector radiator from planetary
and solar heat fluxes, thermal isolation of the radiator from the spacecraft, and
detector bias power dissipation.

In the feasibility study (Reference 1), an experimental model of a radiative cooler
was designed and thermal analyses were performed for a spacecraft in a 200
nautical mile altitude circular earth orbit in the plane of the ecliptic. The cooler
consisted of a primary shield assembly, a secondary shield assembly, a staged
radiator assembly, multilayer insulation assemblies, and support structure; six
design drawings were generated for the experimental model. Based on the detailed
thermal analyses, an orbital temperature of 146°R was predicted for the radiator.

The purpose of the present study was to experimentally verify the thermal per-
formance of the radiative cooler model designed for the 200 nautical mile altitude
orbit. The cooler was fabricated in accordance with the design drawings and pro-
cedures outlined in Reference 1. Tooling was designed and fabricated for use in
fabrication of the cooler. A flat plate, capable of simulating earth albedo and
emission heat fluxes, was also fabricated. The cooler assembly and heat flux
simulator were tested for thermal performance in the 36°R (20°K) Arnold Engineer-
ing Development Center (AEDC) 7V thermal vacuum chamber.

1

A total of four tests were performed. Test conditions varied for these tests were earth simulator temperature and spacecraft skin temperature. The tests produced higher temperatures for the radiator than were predicted. The first stage of the radiator reached a maximum equilibrium temperature of 246°R with the simulator at a temperature of 520°R and the spacecraft skin at a temperature of 560°R; the predicted radiator temperature for this test condition was 156°R. The radiator reached a minimum equilibrium temperature of 200°R with the simulator at a temperature of 140°R and the spacecraft skin at a temperature of 460°R; the predicted radiator temperature for this test condition was 120°R. Based on a correlation of the test and analytical data, the primary reasons for the higher test temperatures were identified as (1) higher than predicted thermal conductances between the spacecraft structure and the secondary shield assembly and (2) higher than predicted thermal conductances between stages of the radiator and between the radiator base and the spacecraft structure.

SECTION II

PROGRAM DESCRIPTION

2.1   OBJECTIVES AND REQUIREMENTS

The primary objective of the subject program is to verify and evaluate the
thermal design of the development configuration of a model radiative cooler
by a thermal vacuum test. The cooler consists of a staged radiator as-
sembly, a primary shield assembly, a secondary shield assembly, multi-
layer insulation assemblies, and support structure (including a portion of
a simulated spacecraft). Basic requirements are as follows: (1) thermal
tests will be performed in a thermal-vacuum chamber with 36°R (20°K)
heat sink walls; (2) planetary fluxes will be simulated by a flat plate earth
simulator; and (3) external heat inputs will be based on the development
design configuration in a 200 nautical mile earth-oriented circular orbit
in the plane of the ecliptic.

Specific requirements for the program are as follows:
Preparation of Radiating Surfaces. The radiator and shield were pre-
pared in accordance with the requirements given in Reference 1. Of
particular concern for the shields were (1) specularity and (2) surface
waviness.
Thermal Insulation. The basic insulation between the shield assemblies
and simulated spacecraft skin was crinkled aluminized mylar, 1.12-in
thick.
Simulated Spacecraft. The simulated spacecraft skin was provided with
heaters to allow variation of skin temperature from 460°R to 610°R.
Earth Heat Flux Simulator. Radiant earth albedo and emission heat
fluxes incident on the configuration were simulated by a flat plate con-
figuration provided with surface heaters. A 4-ft by 4-ft square plate
simulates the view factor between earth and the configuration for the
200 nautical mile altitude orbit.
Detector Cell Simulation. The detector power dissipation was simulated
by a precision carbon resistor, capable of dissipating bias power from
5 to 50 milliwatts.
Instrumentation. The cooler and earth heat flux simulator were properly
instrumented to allow the accurate temperature determination and to allow
a comparison of analytical and experimental results. The earth heat flux
simulator was checked and calibrated by a radiometric instrument to
ensure proper heat flux simulation.
Test Chamber. The test chamber had the capability of maintaining its
cold wall temperature at 36°R under full heat load and of maintaining a
vacuum of 10^{-5} mm Hg or higher. Total power input to the cooler and
earth simulator was limited to 2750 watts maximum. The cooler and
earth simulator fitted into a chamber 66 inches in diameter and 110 inches
long.

3

Test Program. Tests were run to evaluate the effect of the following parameters on cooler performance: (1) detector bias power dissipation (5 to 50 milliwatts), (2) spacecraft temperature 460°R to 610°R, and (3) simulated earth albedo and emission energy incident on configuration (representative of 200 nautical mile altitude orbit).

2.2   DESCRIPTION OF COOLER AND EARTH SIMULATOR

For the operation of the subject passive radiative cooler, it was essential to have the following: (1) minimization of external heat loads (from the earth and sun); (2) maximization of the view factor of the detector radiator to deep space; and (3) thermal insulation of the cooler from the remainder of the spacecraft. The overall cooler configuration is shown in Figures 1 and 2; the means by which the cooler operation was attained is discussed below.

The cooler configuration is located on the spacecraft such that the heat load to the configuration from the earth and the sun is minimized. For an earth-oriented, cube-shaped spacecraft in a 200 nautical mile altitude in the plane of the ecliptic (Figure 3), either surfaces 5 or 6 receives the minimum incident heat flux. Neither of these surfaces receives direct insolation. Therefore the cooler configuration opening may be placed on either of these surfaces.

The relationship of the cooler with respect to the spacecraft (surface 5 or 6) and the earth is shown in Figure 4 . Both the primary and secondary shields are parabolic in shape, with low emittance, low solar absorptance (aluminum) specular surfaces; specular aluminum surfaces are used to close the sides of the parabolas.

Ray tracing of incident earth energy, energy emitted by the primary shield, energy emitted by the secondary shield, and energy emitted by the radiator is shown in Figure 5; for purposes of clarity, the end shields are not shown. Earth albedo and emission energy is incident on the primary parabola and primary ends; for the specular shield surfaces, the energy that is not absorbed by the shield is reflected above the focus back to space.

The primary purpose of the secondary shield is to present a lower temperature environment for the radiator than would be presented if the radiator viewed the primary parabola shield. No direct earth albedo and emission energy is incident on the secondary parabola and ends. Additionally, any energy emitted by the primary shield, or earth energy reflected diffusely off the primary shield, which is incident on the secondary shield is reflected back above the secondary parabola focus to the primary shield and/or space.

In addition to the attenuation of external heat loads on the radiator and shields, heat loads from the spacecraft are also attenuated. Both the primary and secondary end shields are insulated from the spacecraft by use of crinkled aluminized mylar insulation (aluminized on one side

4

PRIMARY SHIELD END

SECONDARY SHIELD END

PRIMARY SHIELD PARABOLA

SECONDARY SHIELD PARABOLA

SIMULATED SPACECRAFT SKIN

SECONDARY SHIELD INSULATION BLANKET

PRIMARY SHIELD INSULATION BLANKET

FIBERGLASS STRUCTURE

STAGED RADIATOR
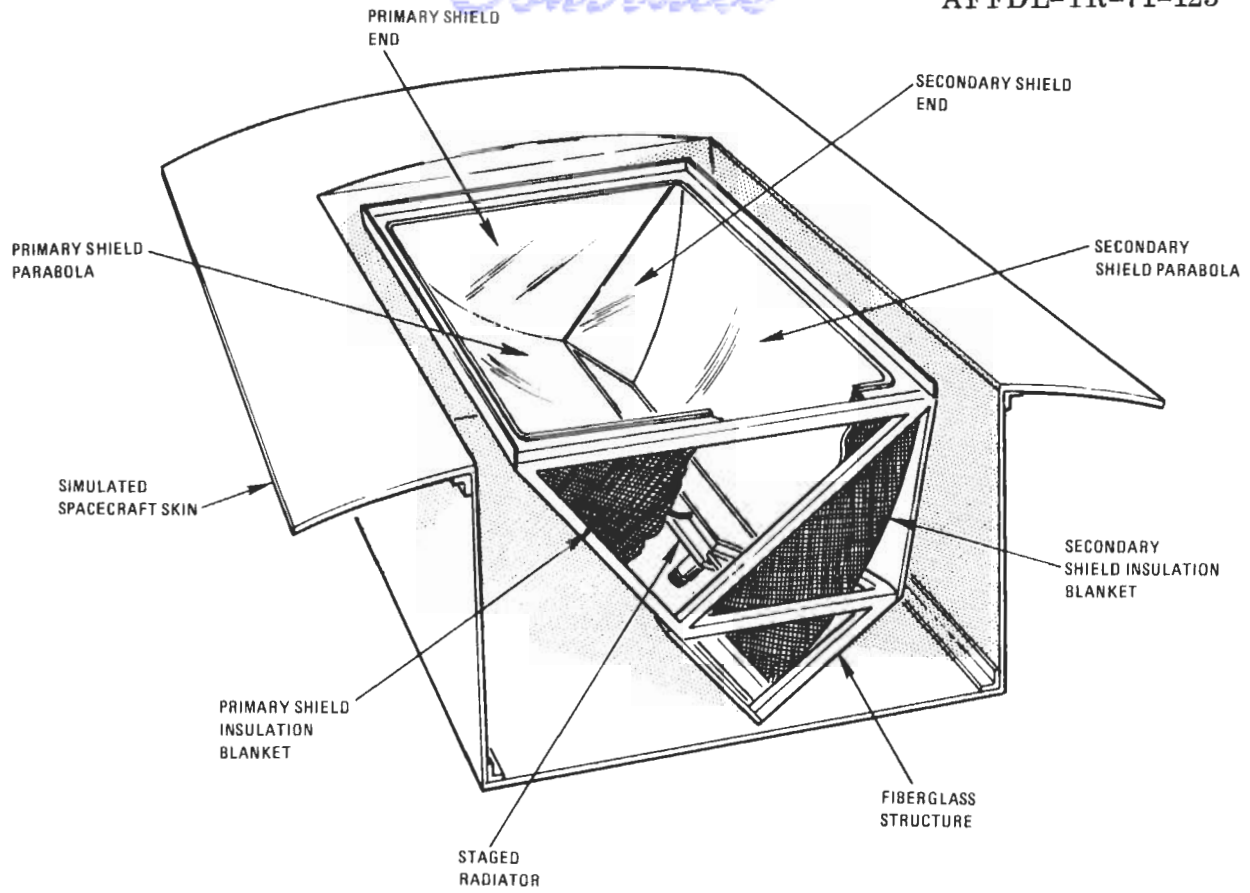
Figure 1 Radiative Cooler Configuration
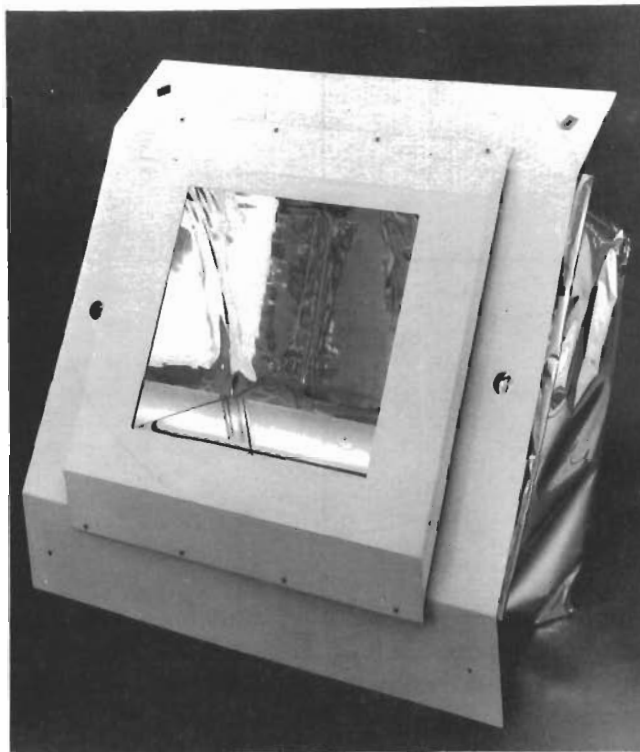
Figure 2 Radiative Cooler
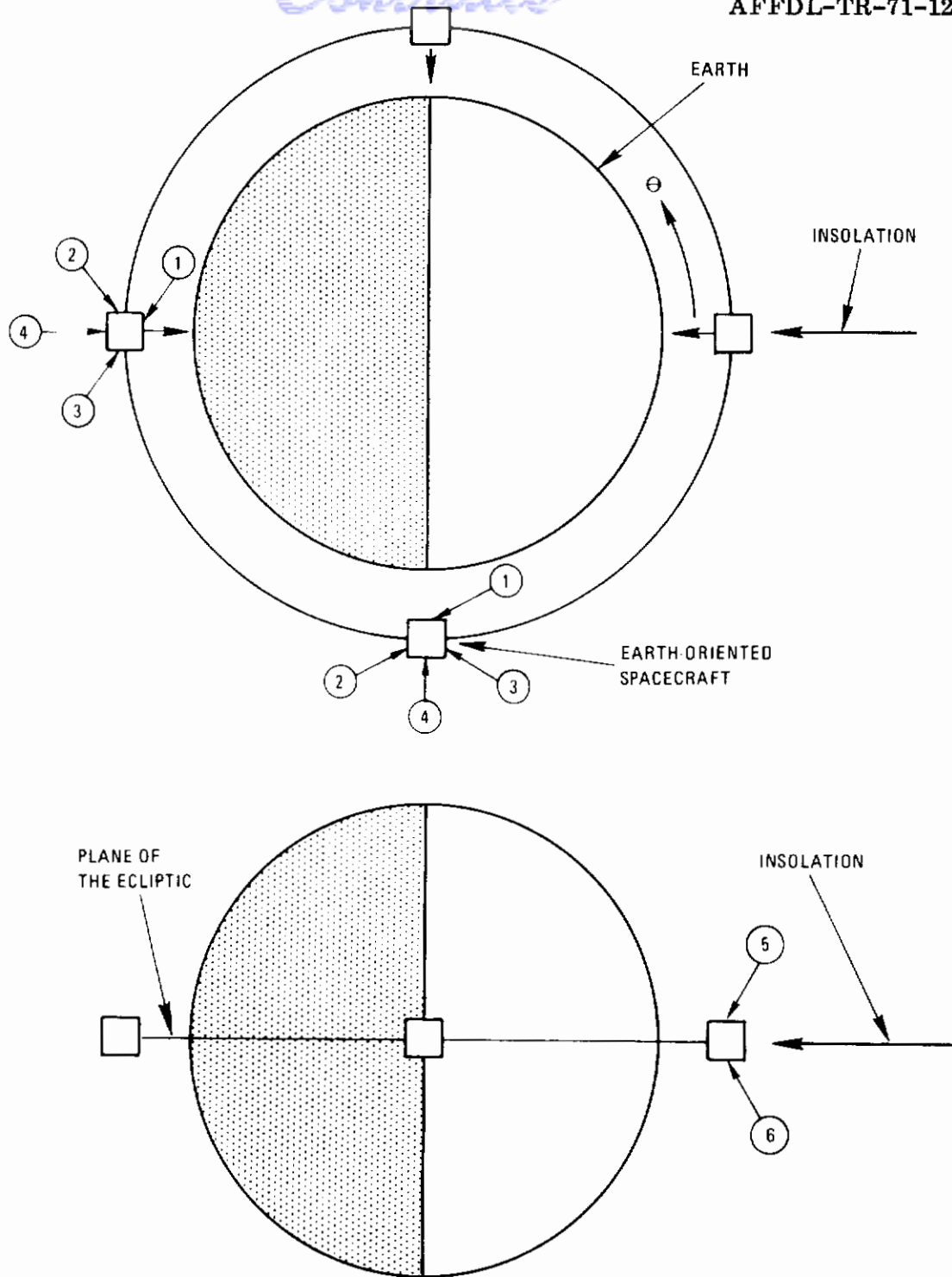
Figure 3
Orbit Description, Spacecraft Orientation, and Surface Definition
of Cubical Spacecraft in an Earth–Oriented 200–nmi
Circular Orbit in the Plane of the Ecliptic

6

LOCATION ON SPACECRAFT

PRIMARY SHIELD (PARABOLA)

SPACECRAFT SURFACE 5 OR 6 (FIGURE 3) (IN PLANE OF ECLIPTIC)

PRIMARY SHIELD PARABOLA ORIGIN AND SECONDARY SHIELD PARABOLA FOCUS

STAGED RADIATOR

EARTH

SECONDARY SHIELD PARABOLA ORIGIN

SECONDARY SHIELD (PARABOLA)

PRIMARY SHIELD PARABOLA FOCUS

CONFIGURATION RELATIONSHIP WITH RESPECT TO INSOLATION, EARTH ALBEDO, AND EARTH EMISSION

ISOLATION

PRIMARY SHIELD

LOCUS OF EARTH ALBEDO AND EARTH EMISSION ENERGY INCIDENT ON CONFIGURATION

STAGED RADIATOR

71°

SECONDARY SHIELD

Figure 4 Relationship of Cooler, Sun, and Earth

7

RAY TRACING OF INSOLATION
OR PLANETARY RADIATION

PRIMARY
SHIELD

EARTH ALBEDO
AND EMISSION

RADIATOR
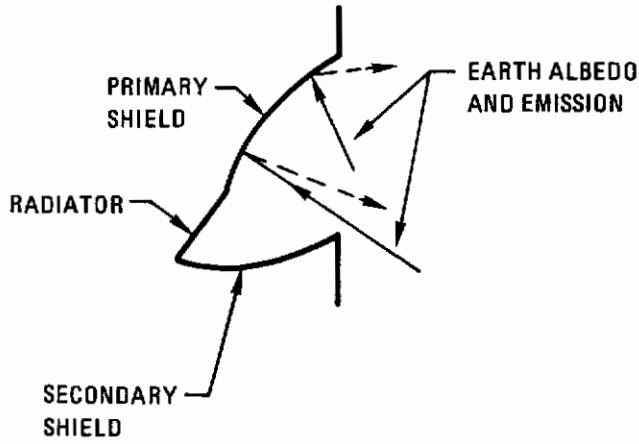
SECONDARY
SHIELD

RAY TRACING OF EMITTED ENERGY
FROM PRIMARY SHIELD

PRIMARY
SHIELD

RADIATOR
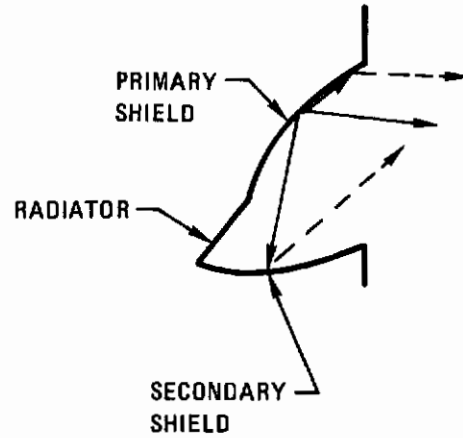
SECONDARY
SHIELD

RAY TRACING OF EMITTED ENERGY
FROM SECONDARY SHIELD

PRIMARY
SHIELD

RADIATOR

SECONDARY
SHIELD
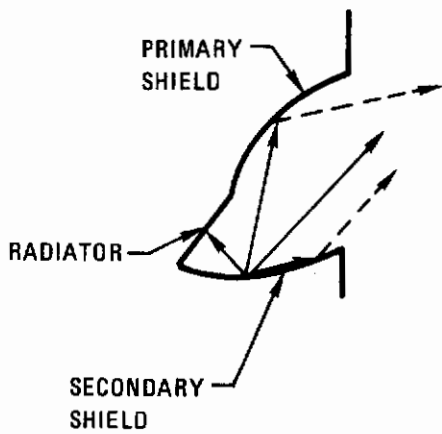
RAY TRACING OF EMITTED ENERGY
FROM RADIATOR

PRIMARY
SHIELD

RADIATOR
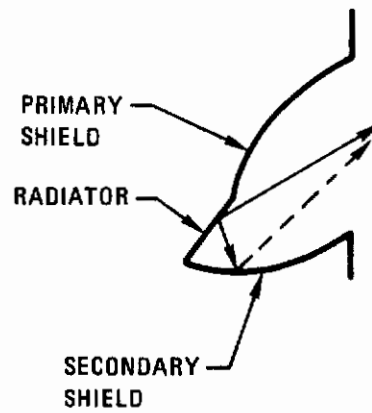
SECONDARY
SHIELD

Figure 5 Energy Ray Tracing of Radiative Cooler

8

only), 1.12-in thick (80 layers per inch). Additionally, low thermal conductance fiberglass pieces are used to insulate the shield assemblies from the structure assembly. The primary and secondary shield assemblies are not conductively coupled to each other. Two-mil and five-mil copper-constantan thermocouple wire is used to measure shield temperatures.

The radiator is thermally insulated from the spacecraft with a staged radiator assembly. Three low emittance (aluminum) stages provide radiative decoupling of the first stage from the spacecraft. Each stage is supported structurally to the next stage via low thermal conductance polyurethane supports. The outboard surface of the radiator is painted white to provide a high emittance surface. Two-mil copper constantan thermocouples are used to measure radiator assembly temperatures.

The primary shields, secondary shields, staged radiator assembly, and insulation assemblies are attached to the fiberglass structure. The fiberglass structure in turn is attached to the simulated spacecraft. The outboard surfaces of the simulated spacecraft are covered with aluminized mylar insulation, in order to reduce heat loads to the chamber. Heaters cover the spacecraft skin, in order to simulate nominal spacecraft temperatures (460 to 610°R).

For the test conditions, earth emission and albedo heating was simulated using a flat 4-ft by 4-ft earth simulator situated in front of the cooler configuration, as shown in Figure 6. The simulator surface facing the cooler opening was painted black. Heaters were bonded to the opposite simulator surface so that the simulator temperature could be attained for the appropriate radiant energy incident on the configuration opening. The heater side of the simulator was covered with aluminized H-film and mylar, so as to reduce heat loads on the chamber.

2.3   PROGRAM PLAN

A flow diagram of the radiative cooler test program is shown in Figure 7. The program consisted of the following tasks:
- Design and fabricate tooling for radiative cooler.
- Fabricate radiative cooler
- Checkout radiative cooler in Philco-Ford 6-ft by 6-ft thermal vacuum chamber
- Design earth simulator
- Fabricate earth simulator
- Calibrate and checkout earth simulator in Philco-Ford 6-ft by 6-ft thermal vacuum chamber
- Test radiative cooler and earth simulator in AEDC 7V thermal vacuum chamber
- Correlate test and analytical data

A detailed description of the program is given in Sections III to VI.

9
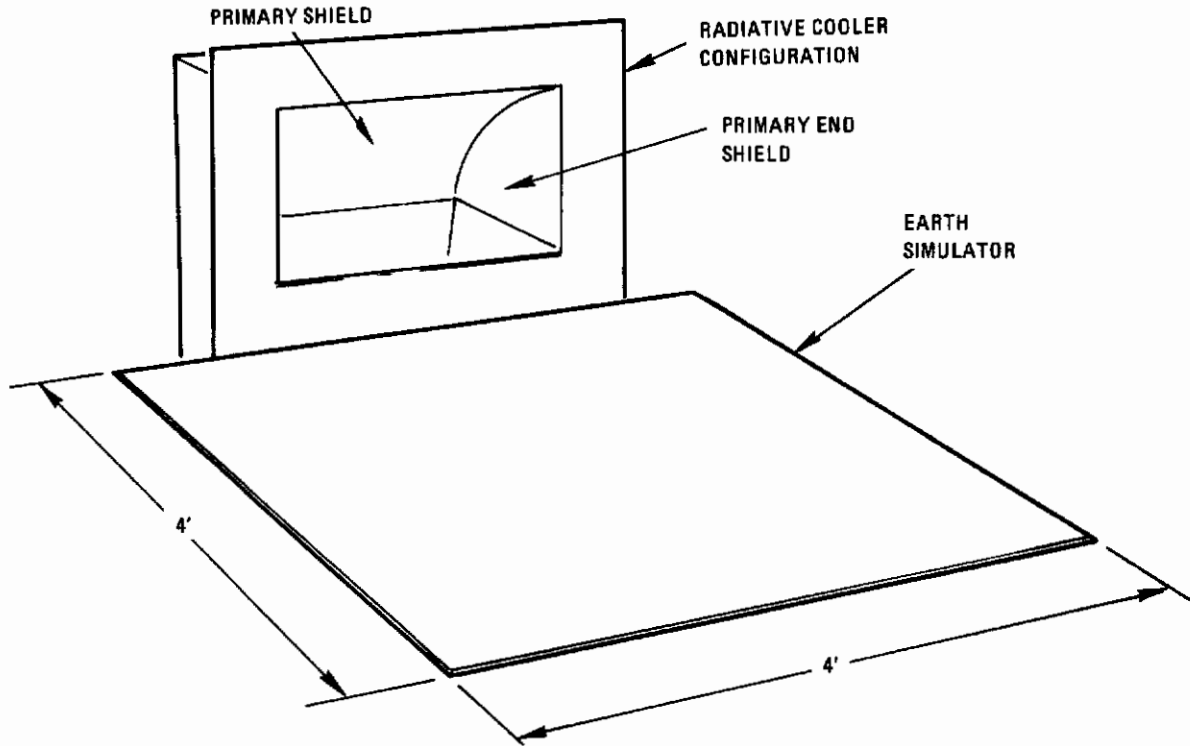
Figure 6 Relationship of Radiative Cooler and Earth Simulator
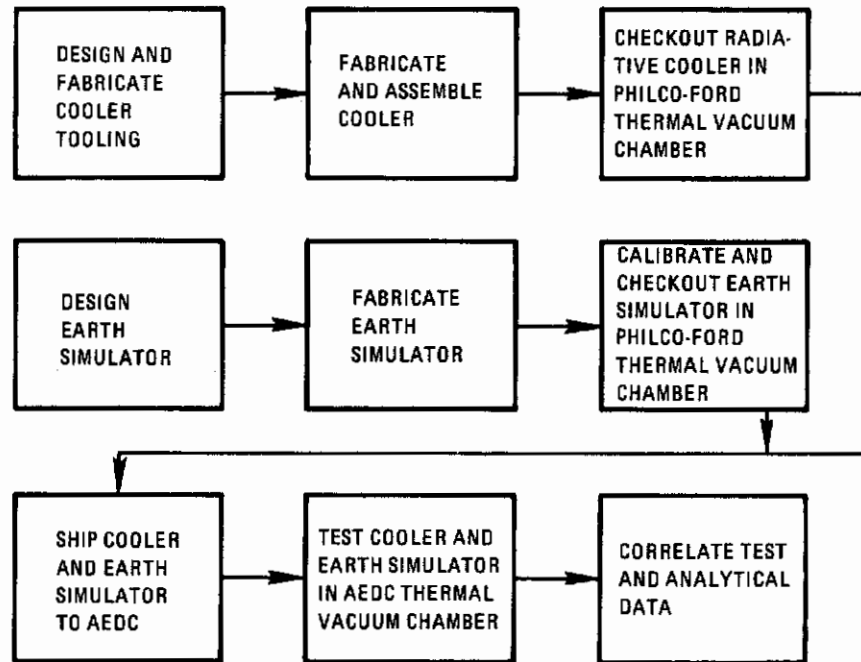
Figure 7 Test Program Flow Diagram

10

SECTION III

COOLER FABRICATION, ASSEMBLY, AND CHECKOUT

The construction of the radiative cooler consisted basically of the following:
- Design and fabrication of the cooler tooling
- Fabrication and instrumentation of the cooler parts
- Assembly of the cooler

Additionally, the optical acceptability was checked out throughout the cooler fabrication, and a thermal vacuum checkout test was performed in the Philco-Ford six-ft by six-ft thermal vacuum chamber prior to shipment to AEDC.

Overall views of the completed cooler are shown in Figures 1 and 2. The individual assembly parts of the cooler and sequence of assembly of the cooler are shown in Figure 8. As described previously in Section II, the cooler consisted basically of the following: a staged radiator assembly, a primary shield (including a parabolic shield and two end shields), a secondary shield (including a parabolic shield and two end shields), a primary shield insulation assembly, a secondary shield insulation assembly, a fiberglass structure to hold the radiator assembly, the two shield assemblies, and the two shield insulation assemblies.

In Paragraphs 3.1 to 3.3, the design and fabrication of the tooling, the detailed design and fabrication, and the instrumentation and assembly of the radiative cooler are described. Additionally, the checkout program for the radiative cooler is described in Paragraph 3.4; described is the checkout criteria and methods for the shield optical surfaces and other thermal control surfaces and the checkout of the cooler in the Philco-Ford six-ft by six-ft thermal vacuum chamber.

The model radiative cooler dimensions, including spacecraft skin, are 36.4 inches wide by 37.4 inches high by 19 inches deep. The dimensions of the cooler opening at the radiative shields are 18 inches wide by 16.06 inches high.

3.1   COOLER TOOLING

Three generic types of tooling were required for the fabrication of the cooler parts: tooling for the primary and secondary shield parabolas, tooling for the secondary shield ends, and tooling for the structural fiberglass parts.

11/12

OUTER FIBERGLASS COVER

SIMULATED SPACECRAFT SKIN

RADIATIVE COOLER

DETECTOR HEATER

FIRST RADIATOR STAGE

POLYURETHANE FOAM SEPARATORS

STAGED RADIATOR SUB-ASSEMBLY

SECOND RADIATOR STAGE

THIRD RADIATOR STAGE

BASE

STRUCTURE ASSEMBLY

SECONDARY SHIELD ASSEMBLY

SECONDARY SHIELD INSULATION ASSEMBLY

PRIMARY SHIELD ASSEMBLY

PRIMARY SHIELD INSULATION ASSEMBLY
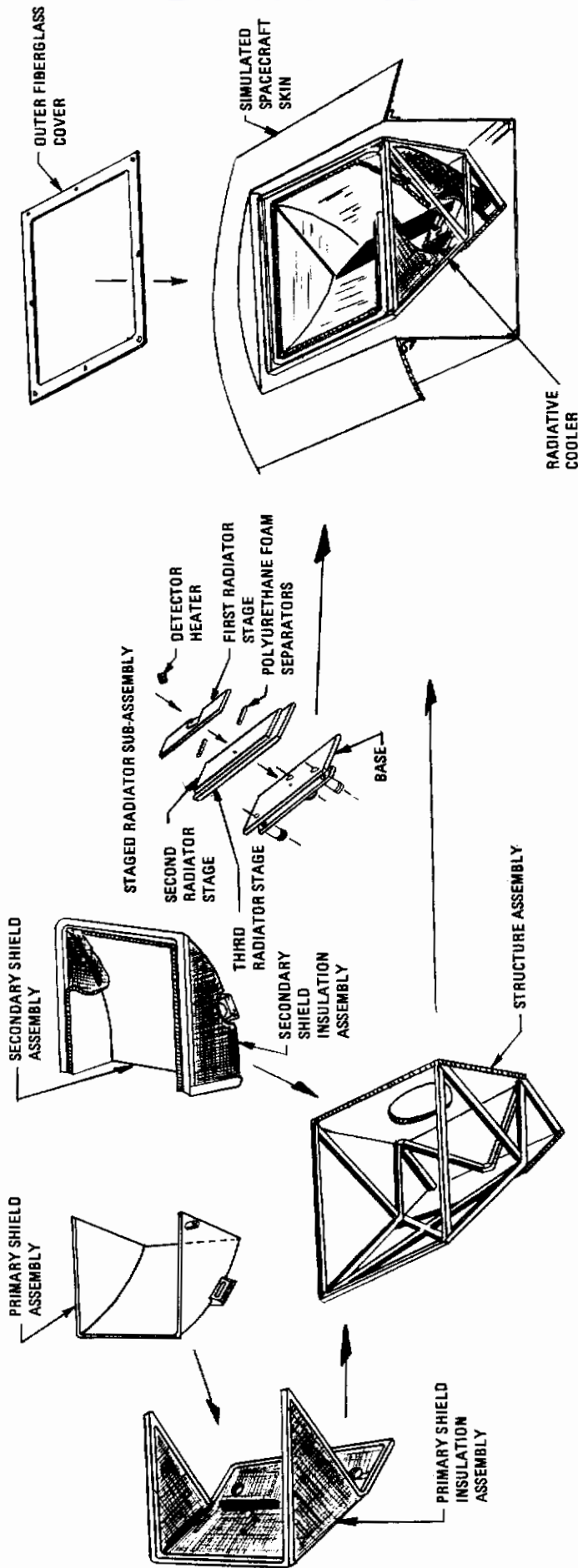
Figure 8 Radiative Cooler Assembly

13/14

3.1.1 Primary and Secondary Shield Parabolas

Two types of tooling were considered for the parabola shield tools: aluminum tools and glass rock tools. As described in Reference 1 and Paragraph 3.4, a most critical aspect of the thermal design of the radiative cooler is the achievement of shield surfaces which meet prescribed specularity and reflectance requirements. Based on roughness and optical measurements performed on sample shield surfaces made on both aluminum and glass rock tools, using the surface fabrication methods described in Paragraph 3.2, either aluminum or glass rock tools could be used for parabola shield fabrication. Therefore, due to schedule limitations, cost limitations, acceptability in obtaining the shield surface requirements, and ease of fabricating the tools, the glass rock tool fabrication method was chosen.

Two glass rock tools were fabricated: the primary parabola shield tool and the secondary parabola shield tool. Each of the tools utilized a fused silica brick base with a slurry coating of silica in water suspension. The fused silica bricks were used as a foundation for the mold. Once the bricks were assembled, the approximate contours of the primary and secondary parabolas were achieved by rough cutting and filing the base of the mold. The silica mold was then mounted in a sweep fixture, which consisted of a knife edged template machined in accordance with primary and secondary shield drawings (Philco-Ford drawings 21-A18714 and 21-A18715). The template was rigidly mounted on two roller bearings riding on a one-inch solid stainless steel bar (Figure 9.).
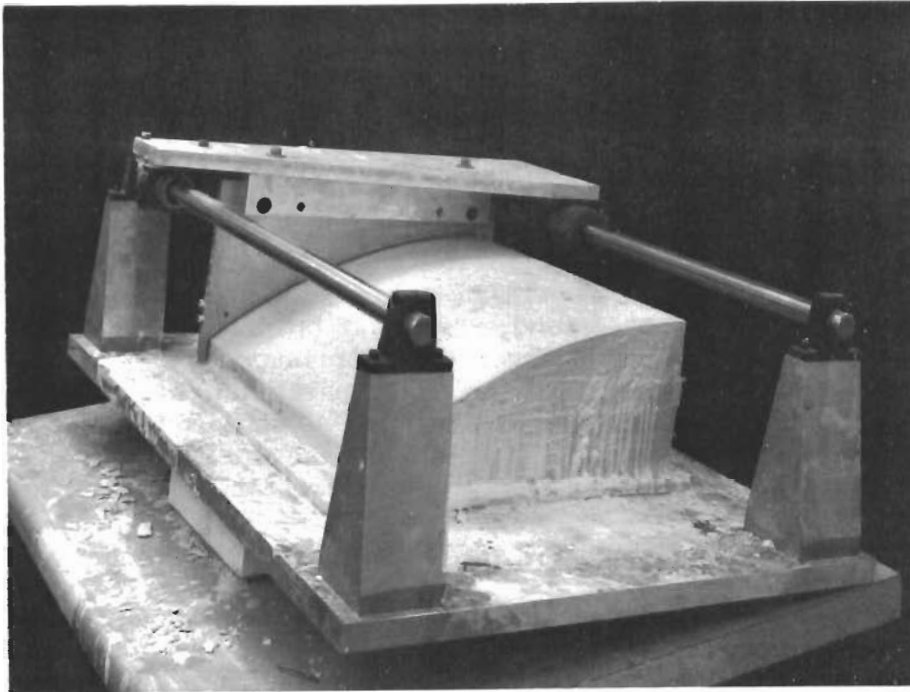
Figure 9 Sweep Fixture for Primary Shield Glass Rock Tool

15

A silica slurry was applied to the mold and successive passes with the template were made until the desired contour and surface finish were achieved.

The sides of the mold were swept in a like manner. In order to achieve parallelism between the two sides, they were both slurried simultaneously. The primary and secondary shield tool molds were allowed to dry for 72 hours at ambient temperature and then post-cured to an ultimate temperature of 785°R for 48 hours. Following the post-cure, the molds were returned to the sweep fixture and the surface was inspected for dimensional unity with respect to the knife edged template. The optically critical surfaces on the mold were then sealed with an epoxy resin and hand polished. The two molds were covered and sealed in a nylon film bag to prevent contamination of the surfaces during storage.

3.1.2   Primary and Secondary Shield Ends

Since the ends for the shield surfaces were flat, flat glass plates were used to lay up the shield ends.

3.1.3   Structural Fiberglass Piece Parts

Aluminum mandrels and tools were used in the fabrication of structural epoxy fiberglass piece parts. The mandrels and tools were fabricated in accordance with Philco-Ford drawings 21-A18714, 21-A18-715, 32-A18717, and 99-A18-718.

3.2   COOLER FABRICATION

The following assemblies were fabricated for assembly into the radiative cooler: radiator assembly, primary shield assembly, secondary shield assembly, primary shield insulation assembly, secondary shield insulation assembly, fiberglass support structure, and simulated spacecraft skin. The assemblies and parts were fabricated in accordance with Philco-Ford drawings 99-A18718 (radiative cooler assembly), 99-A18717 (radiator assembly), 21-A18715 (primary shield assembly), 21-S18714 (secondary shield assembly), 32-A18712 (structure assembly), and DN-A18722 (simulated spacecraft). Of primary concern in the fabrication of the cooler was (1) shield surface preparation (i.e., thermal emittance, reflectance, specularity, and waviness, as outlined in Reference 1 and Paragraph 3.4), (2) thermal isolation of the shields from the spacecraft, and (3) thermal isolation of the radiator from the spacecraft.

3.2.1   Staged Radiator Assembly

The staged radiator assembly consists of three aluminum radiator stages separated by polyurethane spacers and a radiator base assembly. The fabrication of the radiator assembly was based on Philco-Ford drawing 99-A18718. The assembly is shown in Figure 10.

16
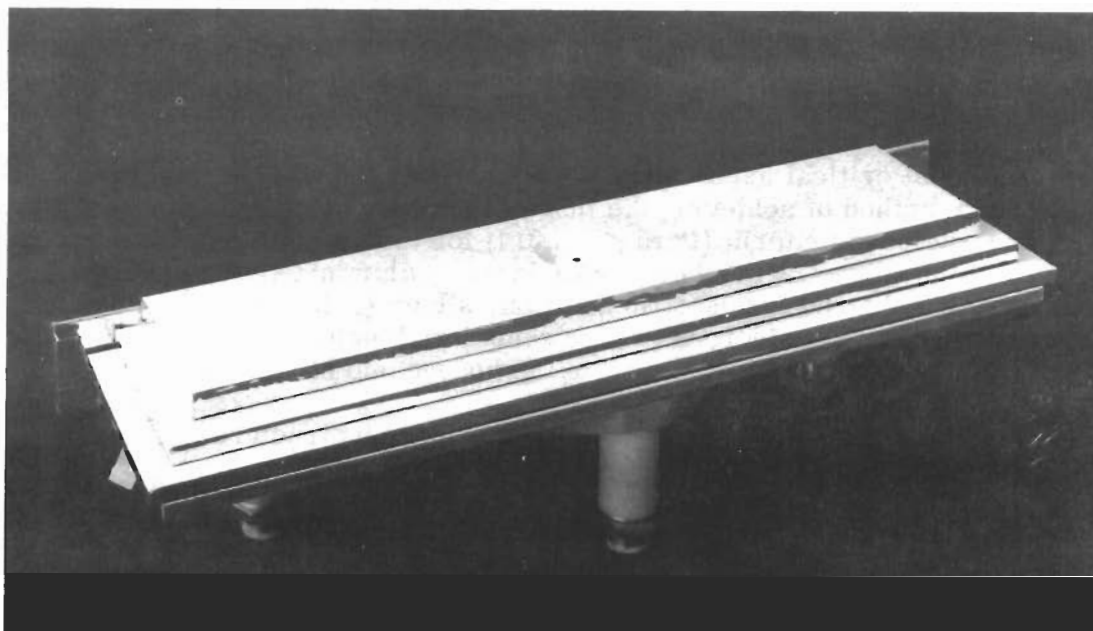
Figure 10 Staged Radiator Assembly

Each radiator stage was fabricated from 20-mil thick aluminum. The size of the stages varied from 3.6 inches by 15.7 inches for the first stage to 4.7 inches by 17.9 inches for the third stage. The surfaces of the stages facing each other were covered by aluminized mylar tape to minimize radiative heat transfer. The surface of the first stage was painted with white Thermatrol paint, which has a room temperature emittance of 0.92.

Following fabrication of the radiator stages, base, and piece parts and the application of thermal control surfaces, the parts were instrumented and assembled. A 50 milliwatt carbon resistor was attached to the first stage, in order to duplicate the thermal dissipation of an infrared detector. A total of nine thermocouples were attached to the radiator assembly; two-mil copper constantan thermocouples were used on all stages. Three thermocouples were attached to the first stage and two thermocouples were attached to the remaining stages. The stages were attached structurally by the bonding of low thermal conductivity, 2 lb/ft^3 density polyurethane spacers to the surfaces, as per drawing 99-A18718.

3.2.2   Primary and Secondary Shields

Based on the requirements of Reference 1 and drawings 21-A18714 and 21-A18715, the primary and secondary shields each consist of a parabola shield and two end shields. The shields consist of a polyamide honeycomb

17

substrate with glass cloth laminate facesheets; a high reflectance, specular aluminum surface was required as the shield surface (front surface) facing the cooler opening. Heaters were required on the shield back surface to prevent contamination of the aluminum surfaces during testing (especially during thermal vacuum chamber cooldown and warmup).

The most critical aspect of the fabrication of the shields was the selection of the method of achieving the thermal emittance, specularity, roughness, and waviness criteria (Paragraph 3.4) for the aluminum or aluminized shield surface. A number of aluminum or aluminized shield surfaces were considered for use. In addition, silver (a thermally acceptable surface) was considered. Those considered included the following:

(1) Aluminized H-film bonded to the honeycomb structure (aluminum side out)
(2) Aluminized mylar bonded to the honeycomb structure (aluminum side out)
(3) Aluminum vacuum deposited on stainless steel
(4) Aluminum vacuum deposited on electroformed nickel
(5) Silver vacuum deposited on stainless steel with an overcoat of Si O_x

Items (3) to (5) were eliminated for this program primarily due to schedule and cost limitations. Therefore the fabrication was narrowed to aluminized mylar and aluminized H-film.

As discussed in Paragraph 3.4, both the mylar and H-film were acceptable in regard to their thermal emittance, specularity, and surface roughness. For both surfaces, the room temperature emittance (as measured with a Lion Model 25 emissometer and Gier Dunkle heated cavity) was 0.04, the specularity (as measured on a Perkin-Elmer model 350 spectrophotometer and a Perkin-Elmer model 13U spectrophotometer) between wavelengths of 2 and 15µ was 97% or higher, and the surface roughness, as measured on a Cleveland roughness indicator, was between 2 and 4 microinches. However, based on visual examination and optical comparator measurements, the H-film surface did not meet the waviness criteria. Upon further investigation, it was determined that the waviness was inherent in all of the H-film sheets during manufacture. Therefore aluminized mylar was chosen for the shield surfaces.

Following the selection of the aluminized mylar, it was determined that the quality of the mylar sheets varied from roll to roll and between sections of each roll. Many of the aluminized mylar rolls or sections of rolls were eliminated on the basis of two common characteristics. The first and most common characteristic for rejection was the presence of a clouded film, which probably was a result of contamination of the surface at the time of vapor deposition. The second most common unacceptable property of many of the films was an irregular or wavy distortion, which was probably caused by either non-uniform rolling of the mylar film or a non-uniform deposition of aluminum. This latter characteristic appeared more prevalent with the films having a thickness greater than 1 mil. Therefore 1-mil thick aluminized mylar was selected as the most acceptable film for use on the shields.

18

A method for obtaining rigidity of the reflective film without loss of optical flatness and reflectivity was developed for this program. The aluminized mylar was mounted on a highly polished glass surface with the reflective side in contact with the glass, under high pressure adhesively bond on a semi-rigid backing. A semi-rigid epoxy resin system was used as the backing material. It was essential that the adhesive be semi-rigid in order that the reflective surface, when secondarily bonded to the honeycomb substrate, would be dimensionally compatible with the parabolic contour. When highly reflective surface was fabricated, it was measured for optimum reflectance on the Lion emissometer and then immediately sealed in an airtight polyethylene bag for protection from contamination.

The honeycomb substrates, upon which the optical surfaces were later mounted, were fabricated by the following procedure. An epoxy impregnated glass cloth laminate was formed over the silica mold tool for the parabolas or glass tools for the end shields and cured under vacuum pressure for four hours at 810°R. These face skins were then post-cured at 860°R to ensure the removal of any residual consensable volatiles. The polyamide honeycomb was slit with a knife blade in a quilted pattern to a depth of 0.25 inch to allow for outgassing from within the honeycomb sandwich. The parabolic honeycomb shapes were then mounted on the primary and secondary molds and heat-formed to the parabolic contour under vacuum pressure for one hour at 785°R, in order to increase the dimensional stability of the final honeycomb sandwich assembly. The epoxy laminate face skins were then prepared for adhesive bonding to the honeycomb. The bonding was carried out on the mold under vacuum with an unsupported epoxy film adhesive, having a 0.007-in thickness and a curing temperature of 710°R. The side panel substrates were also fabricated in a like manner.

The aluminized mylar film with its semi-rigid backing was then secondarily bonded to the primary and secondary parabola panels and the primary and secondary end shields. During the bonding process of the parabolic surfaces, the aluminized surface was protected from scratches by use of a 1-mil thick polished stainless steel sheet over the parabolic mold. The aluminized surface was then placed on the stainless steel and a thin coat of epoxy adhesive was applied to its back surface. The honeycomb substrate was then placed over the surface and the entire assembly was vacuum bagged. This bonding was performed at room temperature in order to minimize dimensional distortion. The side shield aluminized surfaces were bonded to the honeycomb substrate, using a flat glass surface in place of the parabolic mold.

Following bonding of the aluminized mylar substrates to the honeycomb substrates, the side shields were structurally bonded to the parabolic shields under vacuum pressure and while aligned on the respective secondary and primary molds. Three thermocouples were bonded to the back of the parabolic shields and two thermocouples were bonded to the back of each of the end shields (Table 1); 2-mil thermocouples were

19

used on the secondary shield assembly and 5-mil thermocouples were used on the primary shield. Conformal heaters were then bonded to the back surfaces of the shields (Table 2).

The primary shield assembly, following fabrication but prior to the addition of structural parts, and the secondary shield assembly are shown in Figures 11 and 12 respectively. The primary shield assembly is 18 inches wide at the cover opening by 15.1 inches high by 10.7 inches deep. The secondary shield is 18 inches wide by 14.5 inches high by 4.8 inches deep. The acceptability of the shield surface was determined following fabrication using a ruby laser, as described in Paragraph 3.4.

3.2.3 Multilayer Insulation Assemblies

Two multilayer insulation assemblies were fabricated for the radiative cooler shields: the primary shield insulation assembly and the secondary shield insulation assembly. The insulation assemblies, cut to conform to the shape of the shield parabolas and ends, were fabricated using 100 layers of crinkled aluminized mylar, aluminized on one side. Each layer of the assembly, except for the inner and outer layers, was 0.25 mil thick. The inner and outer layers were 2 mils thick. The insulation assemblies were fabricated on molds of the two shield assemblies. At the edge of the multilayer insulation, glass heat felt insulation contained within an epoxy edge clip was used to secure the assembly together and to minimize thermal edge effects for the assembly. The edge clips were bonded to the insulation. Cutouts were provided in the assemblies to allow attachment of the structural assembly to the shields. The inner and outer surfaces of both insulation assemblies were instrumented with copper constantan thermocouples (Table 1).

3.2.4 Structure

The fabrication of the structural support frame was based on the design presented in Philco-Ford drawing 32-A18712. The support frame was fabricated with epoxy impregnated, low thermal conductance glass cloth formed on aluminum tooling and two aluminum honeycomb support skins. Structural piece parts and tools are shown in Figure 13. The assembled structure, with the insulated shield assemblies and shields included, is shown in Figure 14. The shields were supported by the structure using low thermal conductance fiberglass supports which penetrated through the insulation assemblies. The radiator assembly was also supported by the structural frame. The structure was instrumented with seven copper constantan thermocouples.

3.2.5 Simulated Spacecraft

The simulated spacecraft was fabricated in accordance with Philco-Ford drawing DN-A18722. The simulated spacecraft consisted of (1) an aluminum skin used to support the radiative cooler structure and to cover three sides of the cooler and (2) a fiberglass cover. Two

20
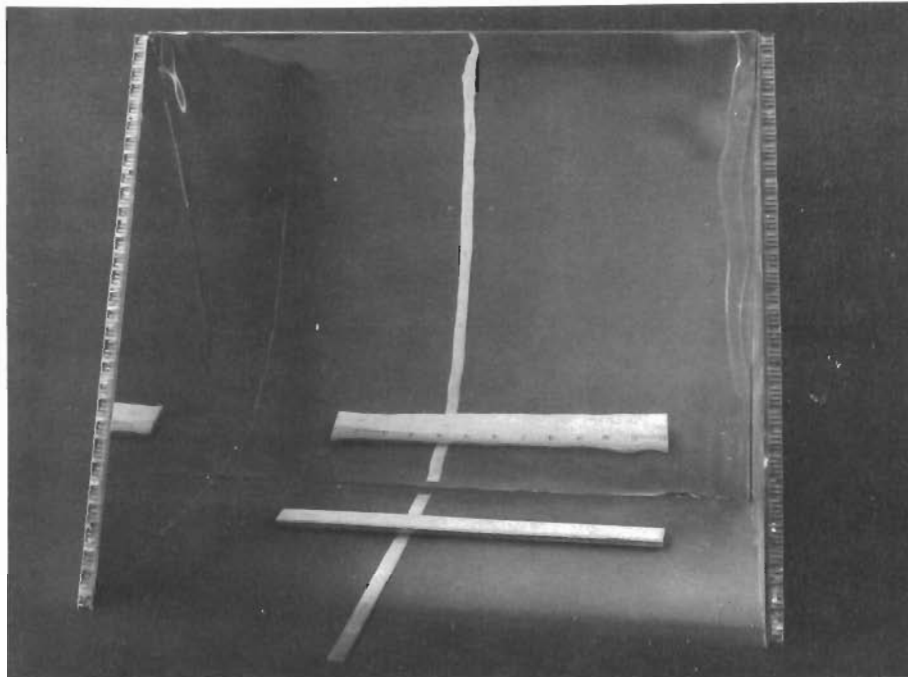
Figure 11 Primary Shield Assembly
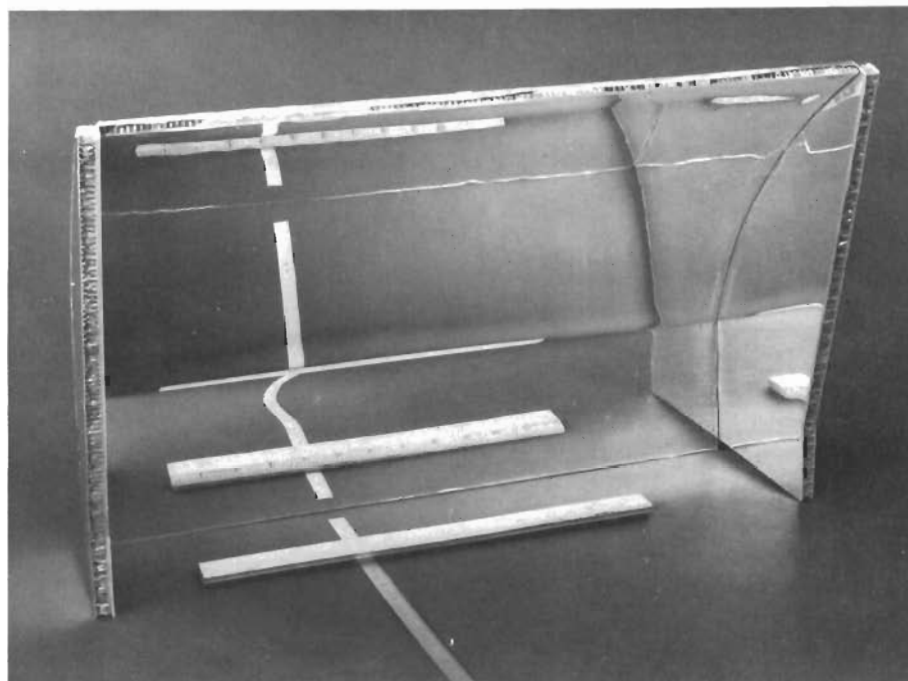
Figure 12 Secondary Shield Assembly

21
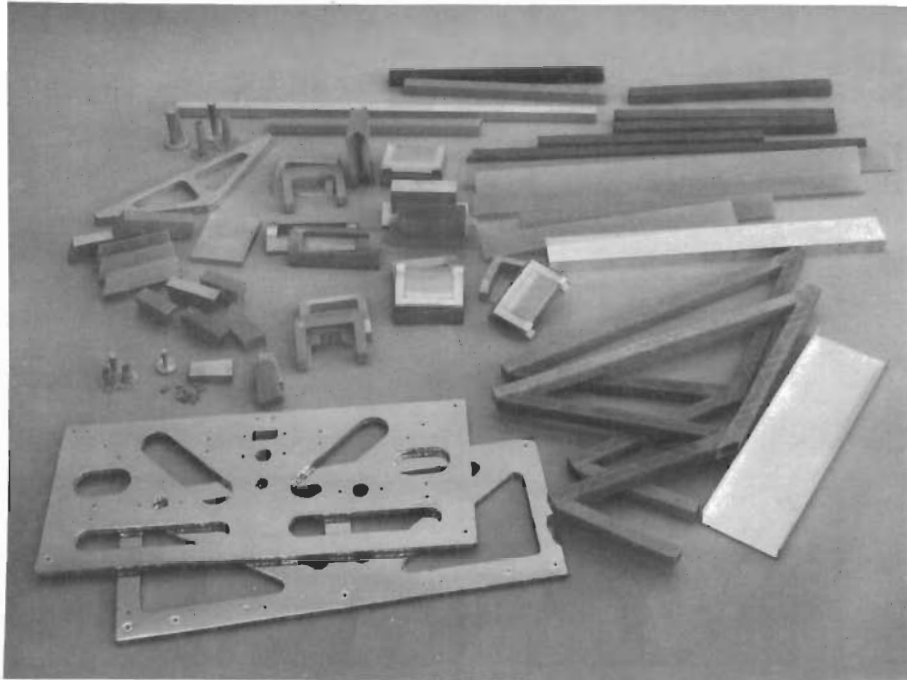
Figure 13 Structure Piece Parts and Tools
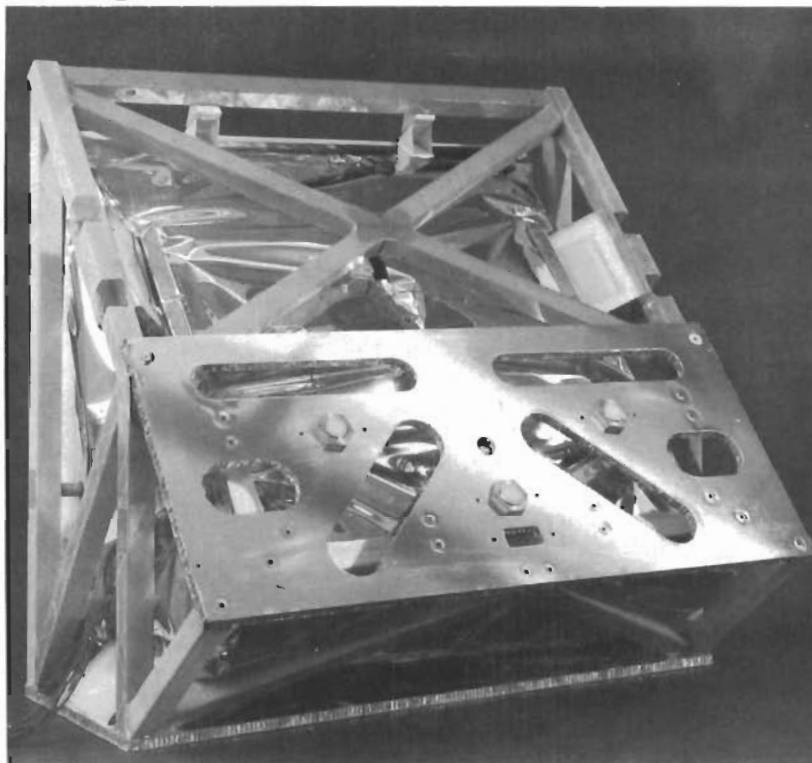
Figure 14   Radiative Cooler Structure

22

conformal type heaters were attached to the aluminum skin of the simulated spacecraft (Table 2). The purpose of the heaters was to maintain the skin temperature between 460°R and 560°R during thermal vacuum testing. The skin was then covered with ten layers of aluminized mylar insulation in order to minimize thermal loads on the chamber during test. Radiation balance calorimeters were attached to the front surface of the skin facing the earth simulator. Ten thermocouples were attached to the aluminum skin.

3.3   ASSEMBLY

Prior to final assembly of the primary shield assembly, secondary shield assembly, insulation assembly, radiator assembly, structure, and simulated spacecraft, all thermocouples and heaters were checked for operation. The assembly sequence of the cooler is shown in Figure 8. The first step of the assembly was to bond the insulation assemblies to the respective shield assemblies. Fiberglass mounting pads were then bonded to the back surface of the shields. The secondary shield was aligned in the structural frame and bonded in position. The staged radiator was then bolted to the honeycomb structural skin. The next step in the assembly was the alignment, mating, and bonding of the primary shield assembly to the structural frame (Figure 15). Prior to final bonding, the alignment was again checked with the ruby laser beam.

For the final step of the assembly process, the structural frame was mounted into the simulated spacecraft.
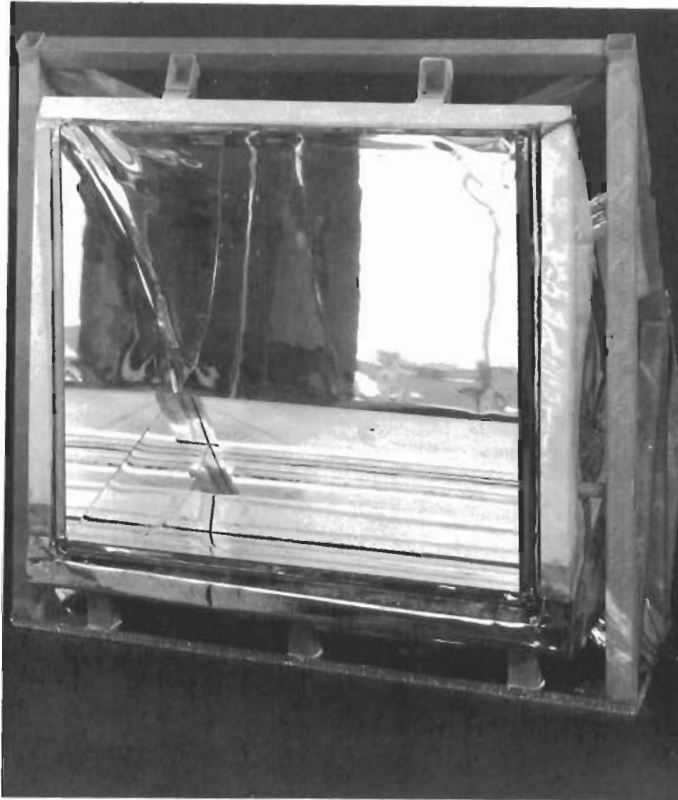
Figure 15
Radiative Cooler Following Assembly of Shields, Radiator Assembly, and Structure

24

3.4   CHECKOUT

The checkout of the radiative cooler prior to, during, and following
fabrication was primarily concerned with the following tests and measure-
ments:

- Determination of the optical and thermal acceptability of various fabri-
  cation methods, materials, and procedures considered for the shields.
- Determination of the optical and thermal acceptability of the shield
  surfaces during fabrication and following assembly.
- Checkout of the cooler in the Philco-Ford 6-ft by 6-ft thermal
  vacuum chamber.

Details of the checkouts outlined above are described in the following
paragraphs.

3.4.1   Shield Fabrication Methods and Procedures

Based on the feasibility study results presented in Reference 1, the pri-
mary requirements for the shield surfaces are the following:

(1)   Room temperature thermal emittance of 0.04 or lower
(2)   Specularity of shield surfaces of 95% or higher for incident earth
        energy.
(3)   Shield surface waviness as defined in Figures 16 and 17.

Based on these requirements, the following criteria were used as
acceptability tests on condidate shield fabrication methods and procedures:

(1)   Total hemispherical room temperature measurements, using both
        a Lion Model 25B Emissometer and a Gier-Dunkle heated cavity.
(2)   Spectral specularity measurements of surfaces between 2 and 15 μ,
        using a Perkin-Elmer model 350 spectrophotometer and a Perkin-
        Elmer model 13U spectrophotometer.
(3)   Roughness measurements of the surfaces, using a Cleveland Model
        BK 6103 roughness indicator. The roughness of a specular surface
        is related to the reflectance by

$$\frac{P_\lambda}{P_{\lambda o}} = e^{\frac{-16 \pi^2 \sigma^2 \cos^2 \theta}{\lambda^2}} \qquad \text{(Reference 2)}$$

where $P_\lambda / P_{\lambda o}$ x 100   is the percentage specularity

σ = RMS roughness (microns)

θ = angle of energy incidence

λ = energy wavelength (microns)

Based on this relationship, the criteria was established that the sur-
face has a 4 microinch (no. 4 finish) or less.

(4)   Optical comparator reading to determine surface waviness.
(5)   Visual inspection

25

SIMPLIFIED TANGENT TO SURFACE

ACTUAL TANGENT TO SURFACE

THEORETICAL
SURFACE

VALLEY

PRIMARY SHIELD
PARABOLA

RADIAL
DEVIATION FROM
TRUE PARABOLA

SECONDARY
SHIELD
PARABOLA

$\Delta \theta$

$\frac{\Delta \theta}{2}$

N'   N

ENERGY FROM EARTH PARALLEL TO EARTH TANGENT/
SPACECRAFT REFERENCE LINE

PEAK

RADIUS OF
TOLERANCE ZONE
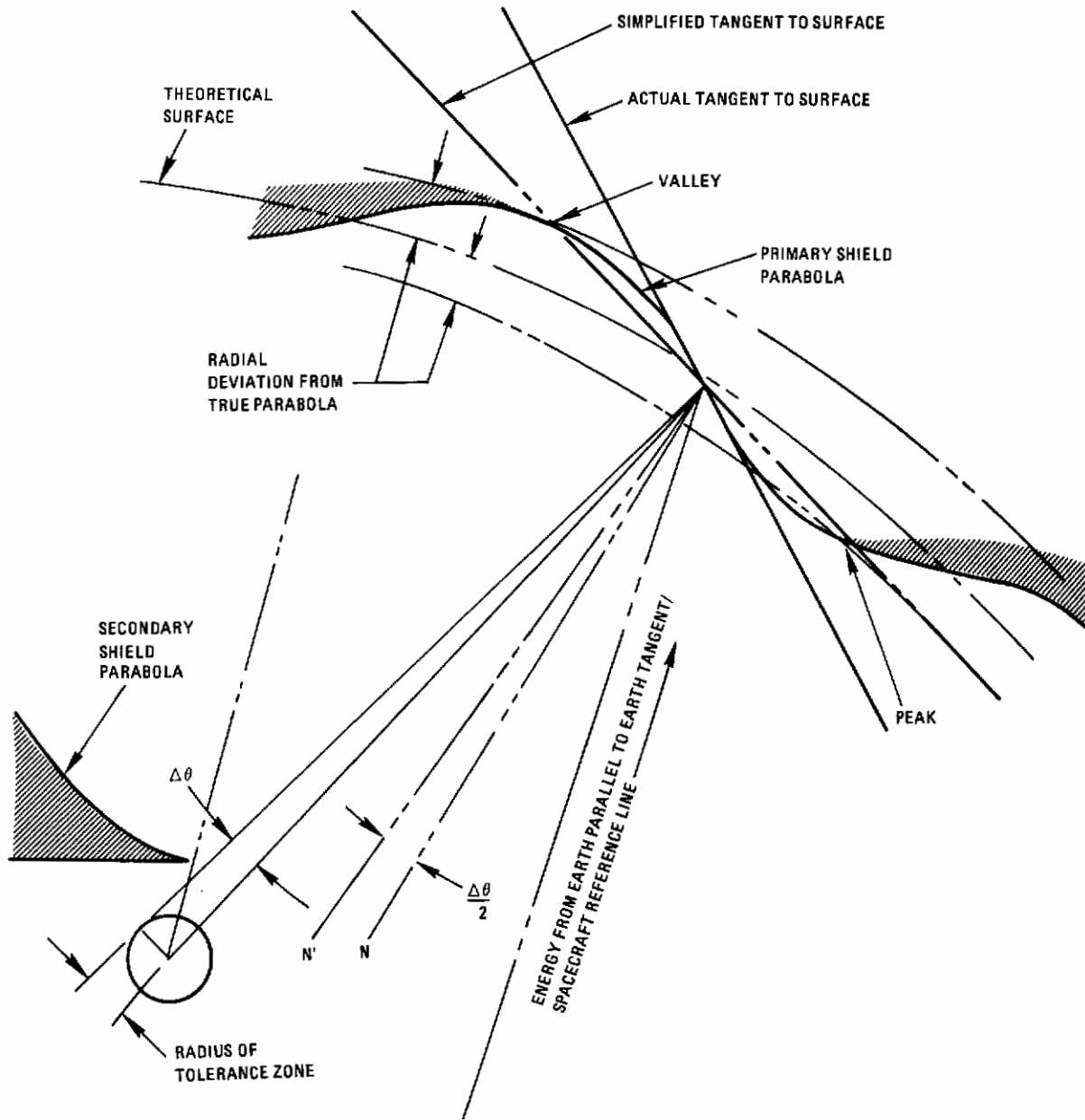
Figure 16   Waviness Geometry- Primary Shield Parabola

26
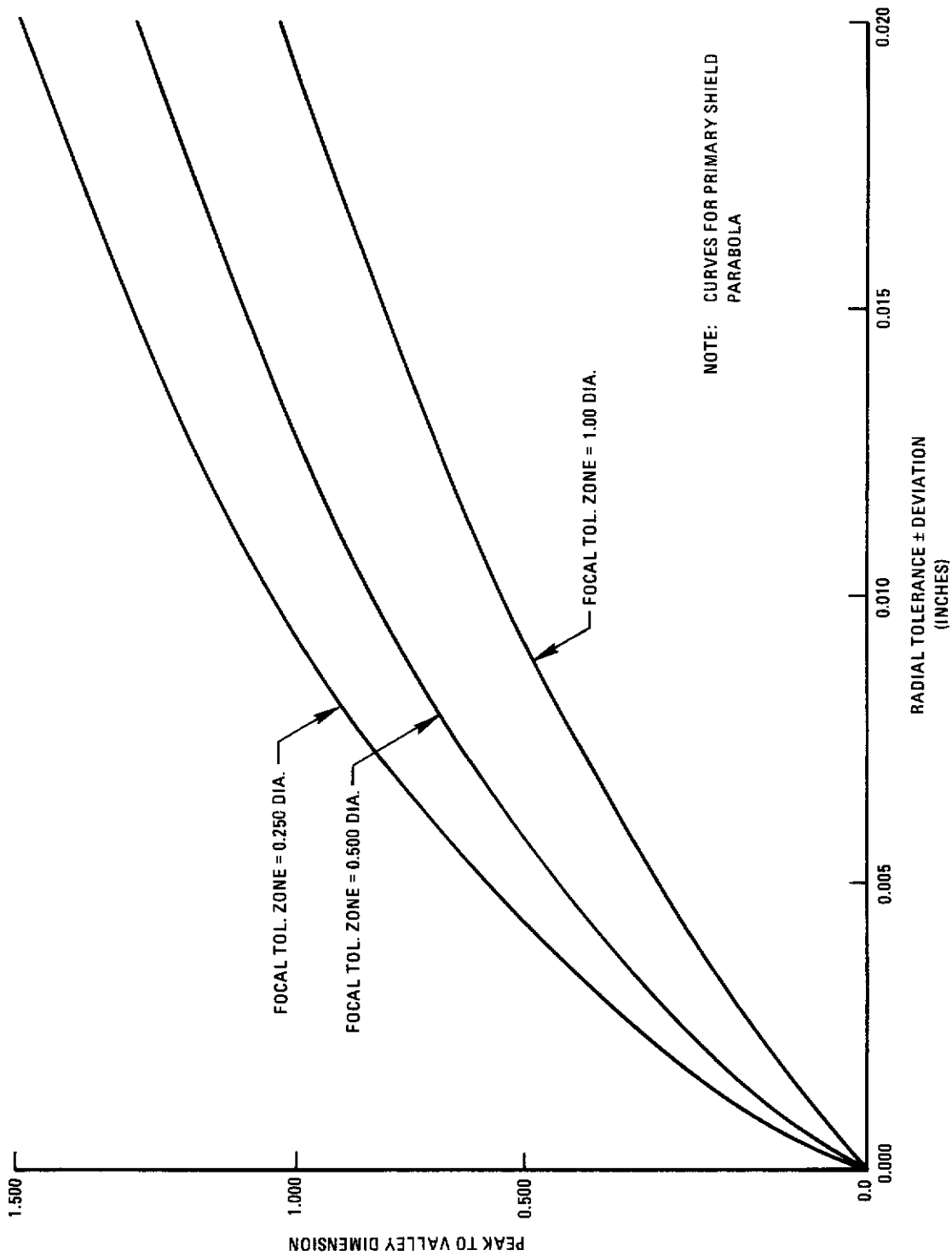
Figure 17

Effect of Parabola Shield Radial Tolerance Deviation on Peak to Valley Dimension

27

As described in Paragraph 3.2, a number of shield surfaces were considered for use. Based on the tests and measurements made on the surfaces, 1-mil thick aluminized mylar was chosen for use as the shield material.

3.4.2 Cooler Fabrication and Assembly

During fabrication of the cooler shield surfaces, the acceptability of the shield was determined using the same criteria, outlined in Paragraph 3.4.1. Following the fabrication of each shield surface, thermal emittance, specularity, and roughness measurements were made on shield samples fabricated with the actual shield surfaces. Therefore no descructive testing was performed on the actual shield surfaces.

Following fabrication, the acceptability of the secondary shield assembly and primary shield assembly were determined by use of an Optics Technology ruby laser beam, 0.25 inch in diameter. The focal plane of the respective shield assemblies were aligned parallel to a horizontally movable optical bench. The ruby laser, vertically movable, was aligned so that its beam was parallel to the focal plane (Figures 18 and 19). A string was then placed across the focus of the respective shields. The shields were then mapped horizontally at 0.5-in intervals in the vertical direction. Based on these measurements, all the reflected energy from the beam was reflected back beyond the focus for the secondary shield assembly. Including two defects in the primary parabola shield, it was estimated that more than 98 percent of the reflected energy from the beam was reflected back beyond the focus and that all the reflected energy was reflected back within 0.5 inch of the focus line. Therefore the shield assemblies were accepted for final assembly.

Following assembly of the cooler assemblies, the alignment of the primary shield with respect to the secondary shield assembly and the radiator assembly were determined using the laser. The focal plane of the primary shield was aligned parallel to the laser beam. The primary shield was again mapped in a similar manner to that described for the primary shield assembly alone. Identical results were obtained as for the primary shield assembly alone; no beam energy was detected on the radiator assembly.

3.4.3 Thermal Vacuum Chamber

Prior to shipment of the radiative cooler to AEDC, the thermal integrity of the cooler was determined in the Philco-Ford 6-ft by 6-ft liquid nitrogen cooled thermal vacuum chamber (Figure 20). The chamber is diffusion oil pumped, with working pressures less than 10^{-5} mm Hg. For the checkout test, the cooler opening plane faced away from the diffusion pump port and toward the liquid nitrogen cooled chamber wall. The pump port was baffled to prevent contamination of the cooler shield surfaces. Additionally, optical mirrors were placed throughout the chamber to monitor any possible contamination.

Figure 18 Laser Beam Checkout of Primary Shield Assembly
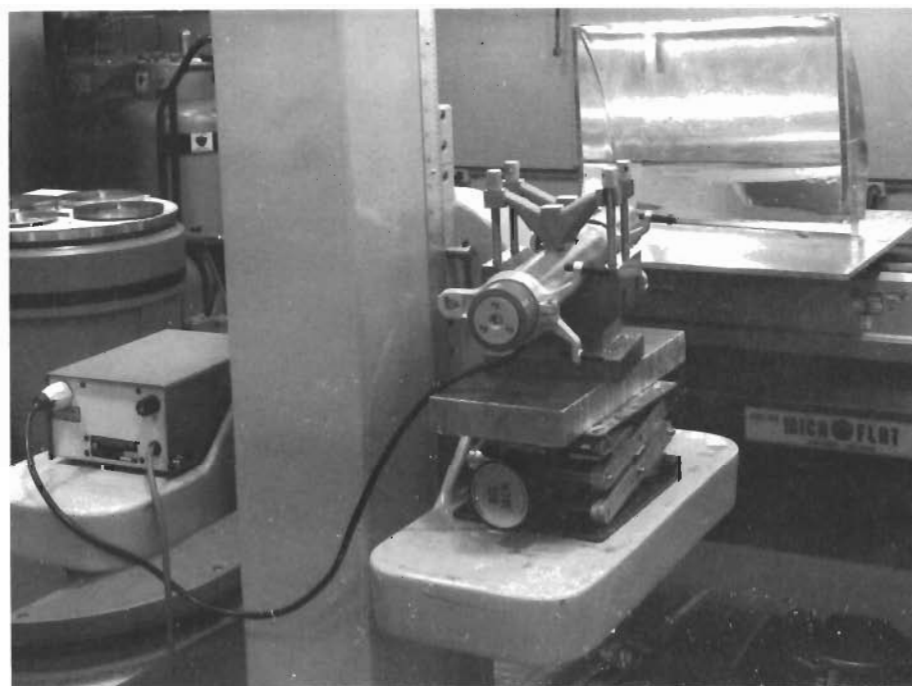
Figure 19 Laser Beam Checkout of Secondary Shield Assembly

29
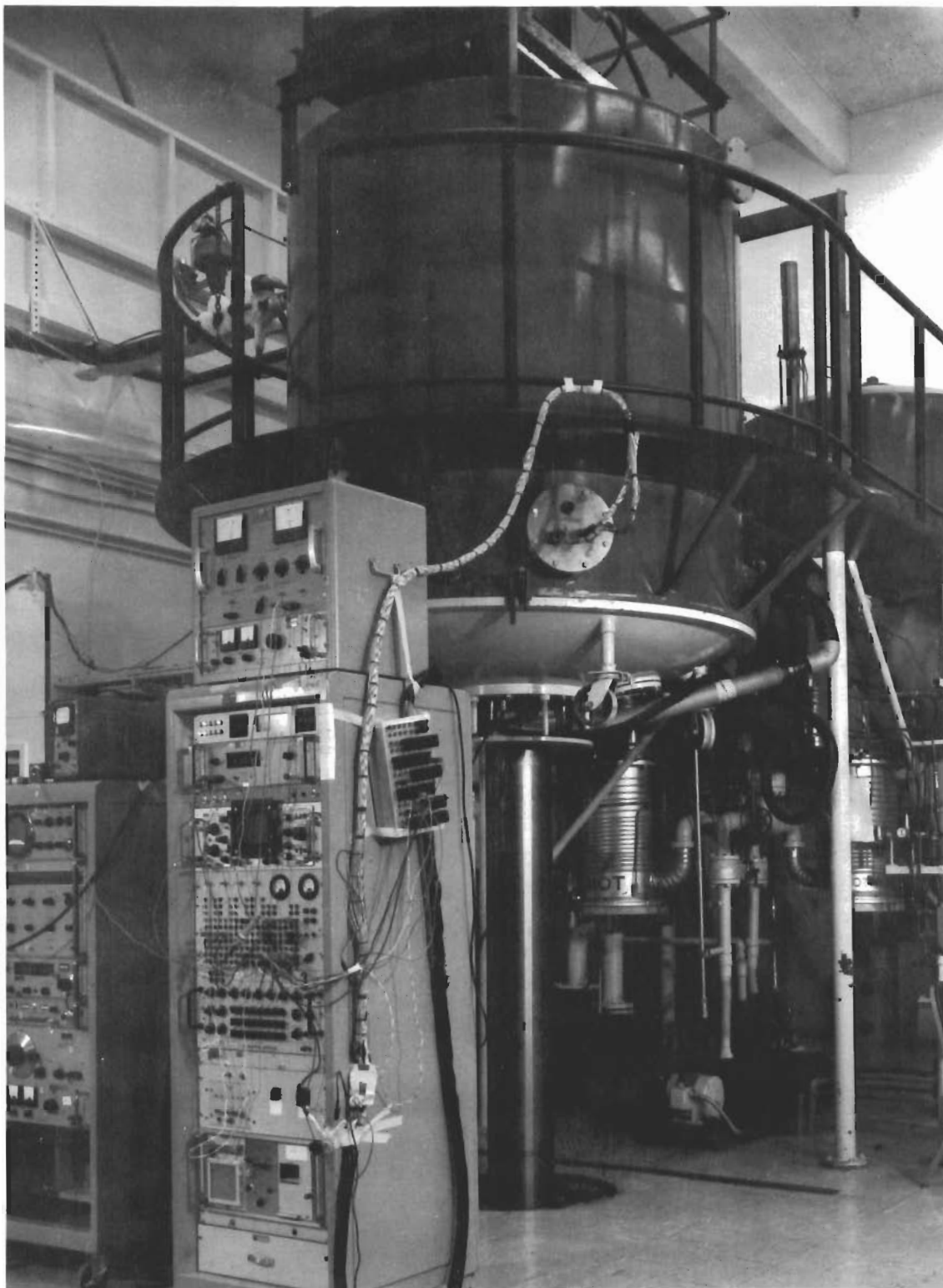
Figure 20
Philco-Ford 6-Ft by 6-Ft Thermal Vacuum Chamber

30

The checkout test was performed with the following conditions: (1) Chamber wall temperature of 140°R; (2) Chamber pressure less than 10^{-6}mm Hg; (3) Spacecraft skin temperature maintained at 460°R; (4) Infrared detector heater dissipation of 10 milliwatts. The earth simulator was not included during the checkout test for the radiative cooler.

The checkout test was performed for a total of sixteen hours. After this period, the first stage of the radiator assembly had reached a temperature of 230°R but had not reached equilibrium. The test was then terminated. Following the test no contamination of the optical mirrors or the shields was noted.

SECTION IV

EARTH SIMULATOR DESIGN FABRICATION, ASSEMBLY, AND CHECKOUT

4.1   DESIGN

The earth simulator design is shown in Figure 21. The simulator con-
sists of a flat aluminum sheet, four feet by four feet by 0.060 inch thick.
3M black velvet paint was used on the top simulator surface in order to
achieve a high emittance, diffuse coating. Five silicone glass sheet
heaters, capable of dissipating a total of 5000 watts energy, are bonded
to the opposite side of the simulator. The purpose of the heaters is to
achieve appropriate temperatures for the simulation of radiant earth
albedo and emission energy. Copper constantan thermocouples are at-
tached to the simulator plate and heaters. A 20-layer insulation blanket,
consisting of layers of aluminized mylar and aluminized H-film, is
attached with high temperature Velcro tape to the simulator, as shown in
Figure 21. The purpose of the insulation is to minimize heat loads on the
chamber.

The primary advantage of this design is its simplicity. Radiant earth
albedo and emission energy is simulated by raising the temperature of
the simulator. The primary disadvantage of the design is that both earth
albedo and earth emission energy is simulated by the infrared energy
emitted by the simulator. Only the earth emission spectrum (energy
peaks at approximately 10μ) is simulated by the simulator at a tempera-
ture of 460°R to 660°R. The earth albedo spectrum (energy peaks at
approximately 0.5μ) is not simulated. Therefore the energy from the
simulator must be adjusted for spectrally selective surfaces, primarily
the aluminized cooler shields, to compensate for different absorptances
to earth albedo and earth emission. For example, the absorptance of
the aluminized shields to earth emission is 0.04 and to earth albedo is
0.12. The simulator heat flux is increased to account for the combined
heat flux of both earth albedo and earth emission energy.

4.2   CALIBRATION AND CHECKOUT

Calibration and checkout of the earth simulator was performed in the
Philco-Ford 6-ft by 6-ft thermal vacuum chamber, with liquid nitrogen
cooled walls. The purpose of this test was to determine the thermal
vacuum integrity of the simulator and to map the emitted simulator
energy in the plane of the cooler opening.

An Eppley thermopile was used to determine the energy incident on the
cooler opening at nine locations of the opening, as shown in Figure 22.
The thermopile was remotely controlled from outside the chamber. The

RADIATIVE COOLER

SECTION 1 (HEATER H89)

SECTION 2 (HEATER H88)

SECTION 3 (HEATER H87)

SECTION 4 (HEATER H86)

SECTION 5 (HEATER H85)

HEATERS

MULTI-LAYER INSULATION

EARTH SIMULATOR PLATE (PAINTED BLACK)
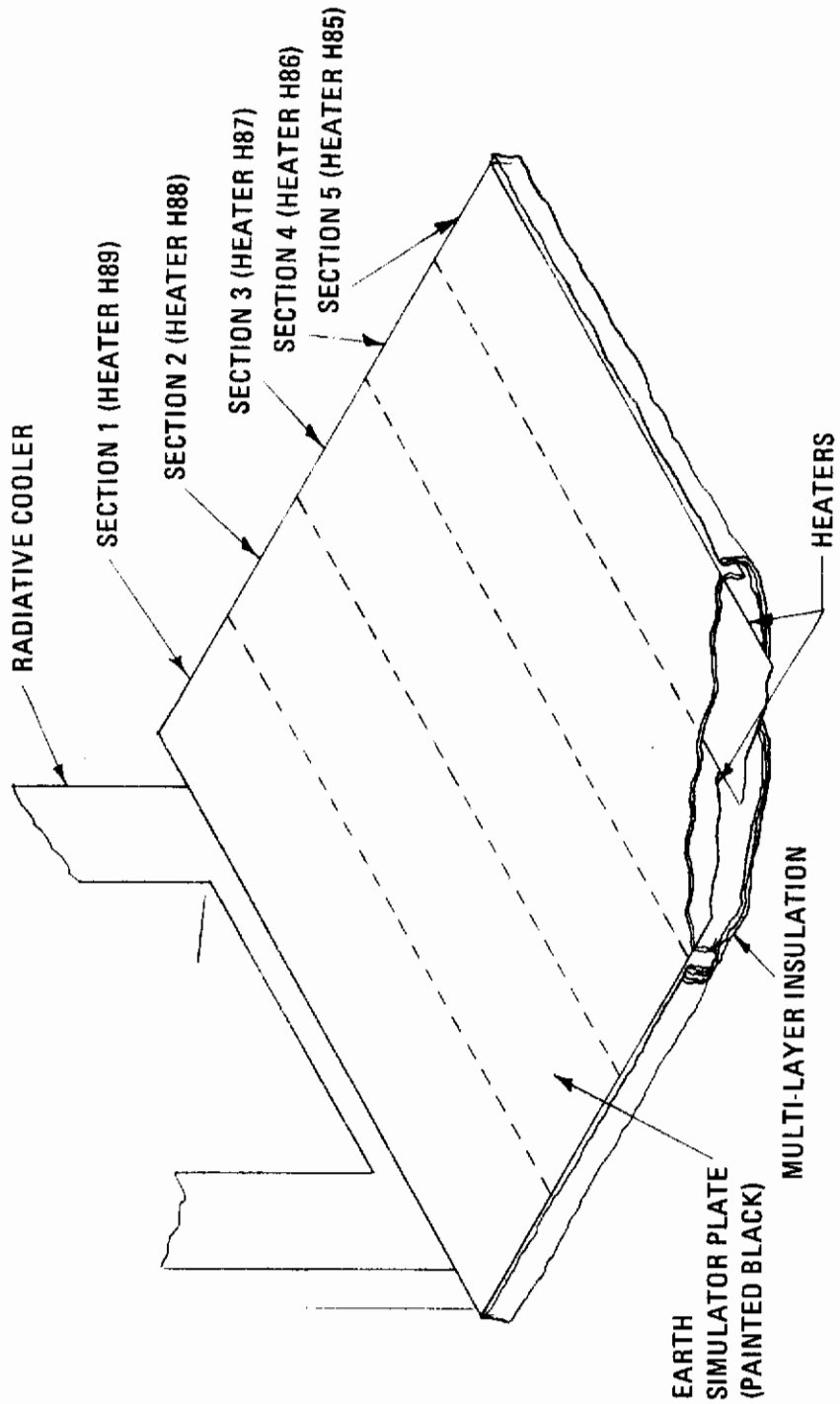
Figure 21   Earth Simulator Design

34
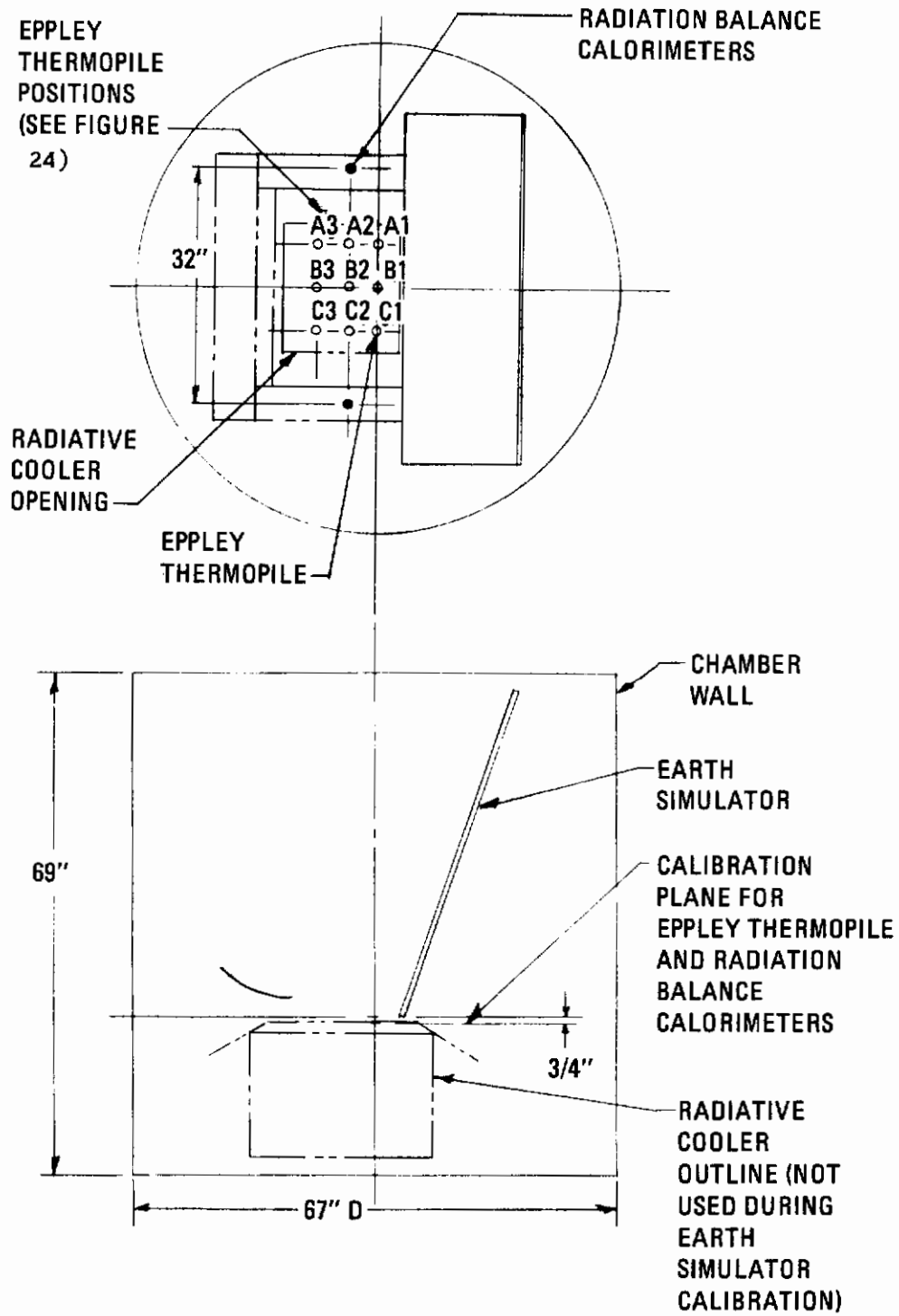
Figure 22 Calibration of Earth Simulator in
6-ft by 6-ft Thermal Vacuum Chamber

incident energy was determined at the nine locations for simulator temperatures between 470°R and 780°R. The incident heat flux varied between 12 Btu/hr-ft^2 at a simulator temperature of 470°R and 115 Btu/hr-ft^2 at a simulator temperature of 780°R (Figure 23). The heat flux map across the cooler opening plane (normalized to an incident flux of 100 Btu/hr-ft^2 at location B1) is shown in Figure 24.

During checkout of the heaters in a vacuum, silicone contamination of the chamber was noted when the heater temperature exceeded 880°R. Therefore as a precautionary measure, the heaters were baked in air at a temperature of 910°R for five days and subsequently baked in a vacuum at a temperature of 810°R for one day. Additionally, the maximum temperature of the heaters during simulator testing was limited to 760°R.
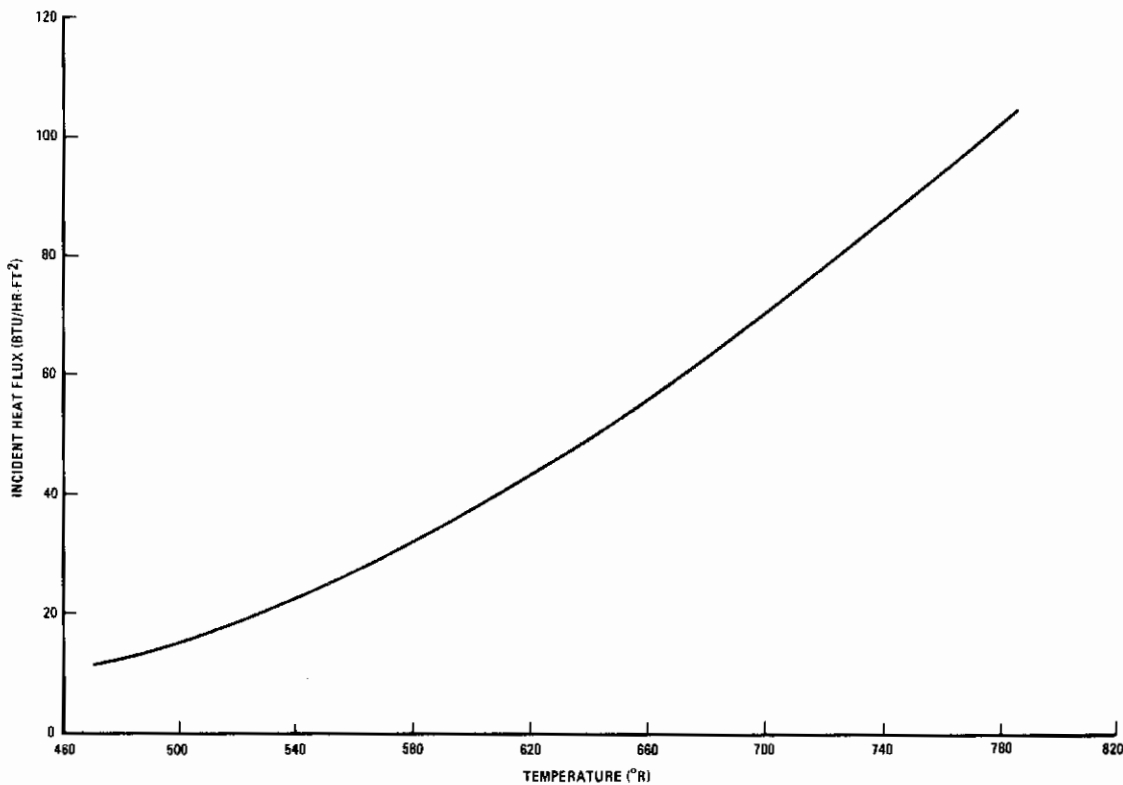
Figure 23 Effect of Earth Simulator Temperature on
Heat Flux Incident on Cooler Opening
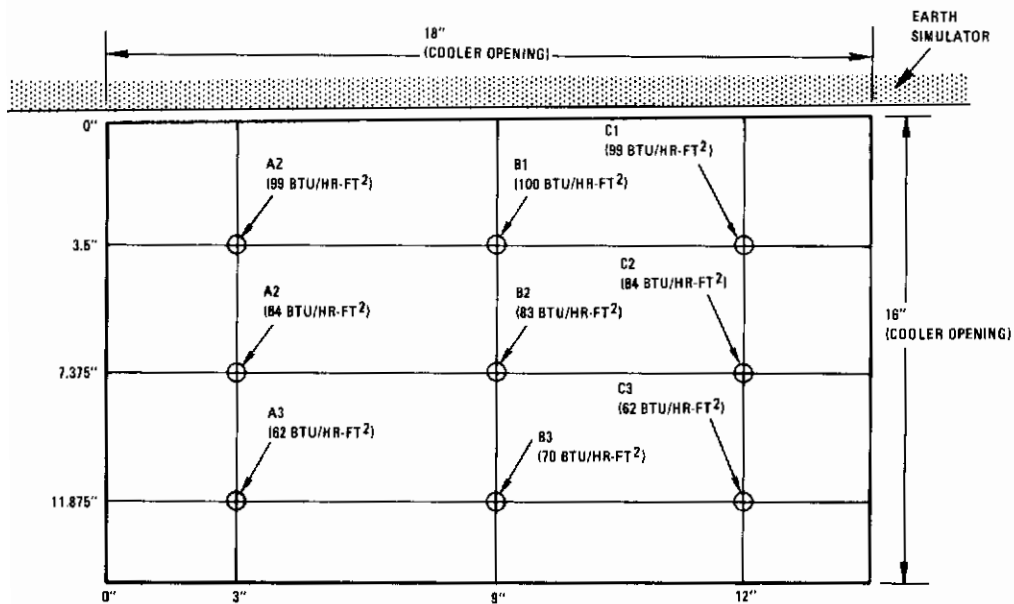
36

Figure 24 Heat Flux Distribution on Cooler Opening Plane

SECTION V

TEST PROGRAM

A total of four tests were performed to evaluate the thermal performance of the radiative cooler. The tests were performed with the spacecraft skin at temperatures of 460°F and 560°R and the earth simulator at temperatures of 140°R (0 Btu/hr-ft^2 energy incident on the cooler opening), 520°R (18.5 Btu/hr-ft^2 energy incident), and 565°R (28 Btu/hr-ft^2 energy incident). An earth simulator temperature of 620°R, representative of energy fluxes for a 200-nautical mile altitude orbit, was not achieved due to unbonding of the earth simulator heaters from the earth simutor. However, the earth simulator temperatures achieved were sufficiently high to evaluate the thermal performance of the cooler. Additionally, effects of infrared detector bias power dissipation were not evaluated due to the failure of the 40-mW detector heater.

5.1 TEST CHAMBER

The subject thermal vacuum tests were performed in the AEDC 7V thermal vacuum chamber. The light-tight chamber, 66 inches in diameter and 110 inches long, has black V-groove helium cooled (36°R) walls throughout. A sketch of the chamber is shown in Figure 25. The walls of the chamber are instrumented with thermocouples and platinum sensors for temperature monitoring.

The location of the radiative cooler and earth simulator in the chamber is shown in Figure 26. The earth simulator plane was located horizontally in the chamber. The cooler was located above the simulator with the angle between the cooler opening plane and the simulator plane equal to 109°. In this manner emitted energy from the simulator was incident only on the cooler primary parabola shield and primary end shields (in addition to the spacecraft skin surfaces). Therefore, the cooler opening viewed the top and sides of the chamber walls, the chamber "West end" door, and the simulator plane itself. The cooler and simulator were attached to the chamber using adjustable low conductance stainless steel wire. The cooler and simulator were aligned with respect to each other and to the chamber dimensionally and visually (i.e., verification that the simulator viewed only the primary shield).

5.2 INSTRUMENTATION AND HEATERS

5.2.1 Radiative Cooler

Three categories of instrumentation were used on the radiative cooler package: thermocouples, heaters, and radiation balance calorimeters.

WEST END
CHAMBER DOOR

BLACK V-GROOVE
WALLS AND DOORS
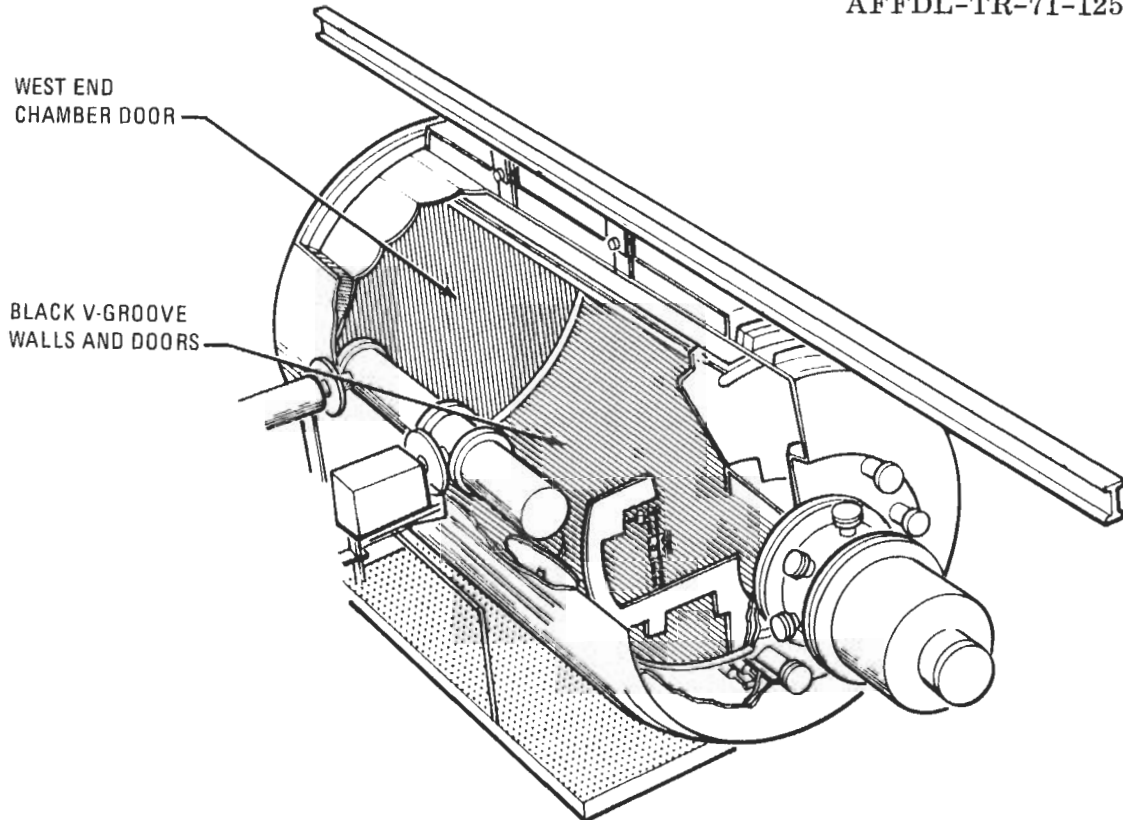
Figure 25 AEDC 7V Thermal Vacuum Chamber
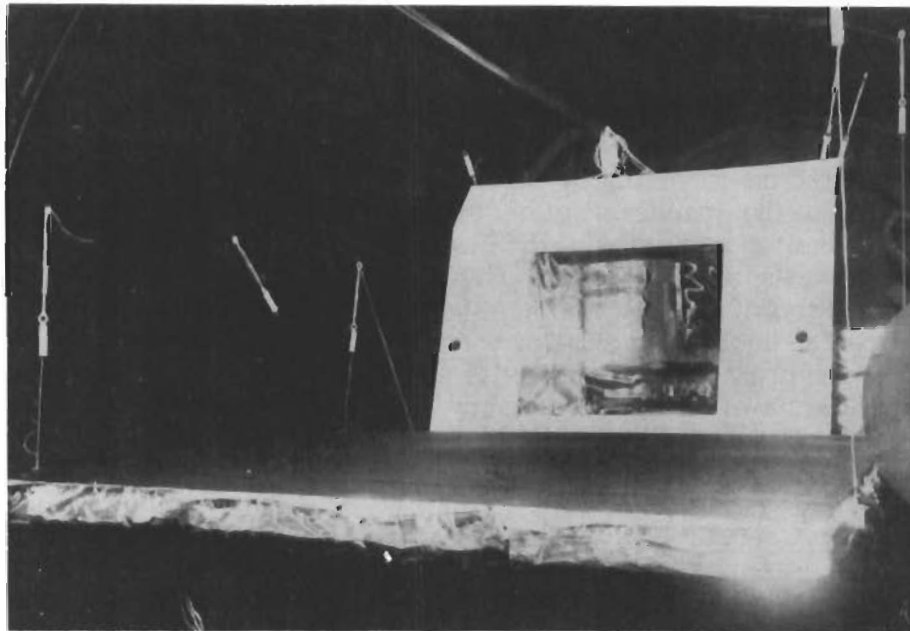
Figure 26 Radiative Cooler and Earth Simulator in AEDC Chamber

40

The purpose of the thermocouples was to monitor the progress of the thermal tests and to determine the thermal performance of the cooler. A total of 52 thermocouples were used on the cooler package. A list of the thermocouples, their locations, and their sizes is given in Table 1. Copper-constantan thermocouples, either 2-mil diameter or 5-mil diameter, were used throughout. Thermocouple location was based on the analytical thermal model of the cooler. Two-mil thermocouples were used where heat leaks were critical to the thermal performance of the cooler, such as on the staged radiator and the secondary shield surfaces. The thermocouple junctions were spot welded to small copper tabs. The tabs in turn were RTV bonded to the proper cooler surface. When attached to a low emittance surface, the thermocouple junction and tab were covered with low emittance aluminized tape.

Three types of heaters were used on the radiator cooler package: shield surface decontamination heaters, infrared detector simulation heater, and spacecraft skin heaters. A list of the heaters used on the cooler, their location, and power rating is shown in Table 2.

A total of six separately controlled decontamination heaters were attached to the honeycomb back side of the six parabolic end shields. The purpose of the heaters was to prevent contamination of the shields from sources within the chamber, including the cooler and simulator, during cool down and warm up of the chamber. The decontamination heaters were added to the cooler based on experience with the contamination of other coolers, both during test and flight. Power to the heaters was adjusted as necessary during chamber cool down or warm up so that the temperature of the shields was maintained between 520°R and 560°R, so as to prevent decontaminants from staying on the shield surfaces. Once the chamber temperatures were stabilized, these heaters were shut off. The heaters were fabricated from Armstrong sheet heaters and were cut from the sheet to fit the shape of the parabolas and ends. Electrical conduction strips and leads were added as necessary to the heaters. The heater lead size was minimized so as to minimize thermal leaks to the shields. After the heaters were covered with polyimide tape to prevent electrical shorting, they were bonded to the back side of each of the shields.

The purpose of the infrared detector heater was to simulate the bias power dissipated by an infrared detector. The heater, a 50 mW carbon resistor, was attached to the first stage (radiator stage) of the radiator. The heater lead size was minimized so as to minimize heat leaks to the radiator. The leads were thermally shorted to each radiator so as to further minimize the heat leaks. Redundant heaters were not used, also so as to minimize heat leaks. As described in Paragraph 5.3, the heater or its leads opened in the cooler during testing and could not be repaired without disassembling the cooler.

Two spacecraft skin heaters were attached by bonding to the aluminum skin of the simulated spacecraft. The purpose of the heaters was to simulate nominal spacecraft temperatures of between 460°R and 610°R.

41

TABLE 1

THERMOCOUPLE LOCATIONS

THERMOCOUPLE NUMBER	LOCATION
1	Primary Shield, Center, Top
2	Primary Shield, Center, Bottom
3	Primary Shield, Side, Bottom
4	Primary Shield End 1, Top
5	Primary Shield End 1, Bottom
6	Primary Shield End 2, Top
7	Primary Shield End 2, Bottom
8	Secondary Shield, Center, Bottom
9	Secondary Shield, Center, Top
10	Secondary Shield, Side, Bottom
11	Secondary Shield End 1, Top
12	Secondary Shield End 1, Bottom
13	Secondary Shield End 2, Top
14	Secondary Shield End 2, Bottom
15	Radiator First Stage, Center
16	Radiator First Stage, Center
17	Radiator First Stage, Center
18	Radiator Second Stage, Center
19	Radiator Second Stage, Side
20	Radiator Third Stage, Center
21	Radiator Third Stage, Side
22	Radiator Base, Center
23	Radiator Base, Side
24	Primary Shield Insulation, Shield Side
25	Primary Shield Insulation, Spacecraft Side
26	Primary Shield End 1 Insulation, Shield Side (Opposite TC4)
27	Primary Shield End 1 Insulation, Spacecraft Side
28	Primary Shield End 2 Insulation, Shield Side (Opposite TC6)
29	Primary Shield End 2 Insulation, Spacecraft Side
30	Secondary Shield Insulation, Shield Side (Opposite TC8)
31	Secondary Shield Insulation, Spacecraft Side
32	Secondary Shield End 1 Insulation, Shield Side (Opposite TC11)
33	Secondary Shield End 1 Insulation, Spacecraft Side
34	Secondary Shield End 2 Insulation, Shield Side (Opposite TC13)
35	Secondary Shield End 2 Insulation, Spacecraft Side
36	Spacecraft Back, Top
37	Spacecraft Back, Bottom
38	Spacecraft Left Side, Top
39	Spacecraft Left Side, Bottom
40	Deleted
41	Deleted
42	Spacecraft Bottom
43	Spacecraft Right Side, Bottom
44	Spacecraft Right Side, Top
45	Spacecraft Top
46	Spacecraft Top Wing
47	Spacecraft Bottom Wing
48	Structure Top Base, Center
49	Structure Top Base, Side
50	Structure Bottom Base, Side
51	Structure Bottom Base, Center
52	Fiberglass Structure, Side
53	Fiberglass Structure, Center
54	Fiberglass Structure, Side

42

TABLE 2

RADIATIVE COOLER HEATERS

HEATER	LOCATION	PURPOSE	THERMOCOUPLE MONITOR	POWER RATING
H-81	Simulated Spacecraft Skin (sides)	Maintain normal spacecraft skin temperature between 460°R and 610°R	38 and 39, 42 to 45	120 Volts, 400 Watts
H-82	Infrared Detector	Simulate infrared detector bias power dissipation	15 to 17	50 Milliwatts
H-83	Simulated Spacecraft Skin (back)	Maintain nominal spacecraft skin temperature between 460°R and 610°R	36 and 27	120 Volts 180 Watts
H-90	Secondary Parabola Shield	Decontamination Heater	8 to 10	50 Volts, 5 Watts
H-91	Secondary Shield, End 1	Decontamination Heater	13 and 14	20 Volts, 3 Watts
H-92	Secondary Shield, End 2	Decontamination Heater	11 and 12	20 Volts, 3 Watts
H-93	Primary Parabola Shield	Decontamination Heater	1 to 3	90 Volts, 7 Watts
H-94	Primary Shield, End 1	Decontamination Heater	4 and 5	40 Volts, 4 Watts
H-95	Primary Shield, End 2	Decontamination Heater	6 and 7	40 Volts, 4 Watts

43

The heaters used were flexible thermo-sheets. Spacecraft heater H81 consisted of four heaters wired in parallel and attached to the four sides of the spacecraft skin. Heater H83 was attached to the back surface of the spacecraft skin.

Two radiation balance calorimeters were attached to the sides of the space-craft skin facing the earth simulator, as shown in Figure 26. The purpose of the calorimeters was to monitor heat fluxes incident on the cooler opening. The calorimeters were calibrated during calibration of the earth simulator, as described in Paragraph 4.2. Each calorimeter consists basically of a disc which is coated black on one side, to absorb the heat fluxes from the heat source, and is thermally isolated by low emittance radiation discs facing the opposite disc side. The temperature of the calibrated calorimeter increases as the incident heat flux increases. YSI thermistors are used to monitor the disc temperatures.

5.2.2   Earth Simulator

Both thermocouples and heaters were used on the earth simulator. The purpose of the thermocouples was to monitor the temperature of the simulator radiating surface and to monitor the heater temperatures. A total of 15 five-mill diameter copper constantan thermocouples were used on the simulator, ten on the radiating surface and five on the heaters. The thermocouples were bonded with RTV directly to the back side of the radiating surface and heaters. A list of the thermocouples and their locations is shown in Table 3.

The purpose of the earth simulator heaters was to control the temperature of the simulator radiating surface. Two separately controlled heaters, H86-89 and H85, were used. Heater H86-89 actually consisted of four separate heaters, wired in parallel. The heaters used were silicone fiber-glass heaters, dimensionally sized so as to cover the entire back surface of the simulator and provide uniform heating of the simulator. A list of the heaters, their location, and their power size is given in Table 4. Each of the heaters was bonded over nearly its entire surface to the back side of the simulator, so as to minimize temperature gradients between the simulator and heater.

5.3   TEST PLAN

The radiative cooler test plan was designed to evaluate the cooler thermal performance, specifically in the following areas: (1) thermal radiative performance of the shield surfaces; (2) thermal isolation of the shields and radiator from the spacecraft; and (3) effect of infrared detector bias power dissipation on radiator temperatures   (Reference 3). Due to the failure of the infrared detector heater and limitations in the test schedule and costs, the number of tests was limited to four and the effect of de-tector bias power dissipation on radiator temperatures was not evaluated.

TABLE 3

THERMOCOUPLE LOCATIONS ON EARTH SIMULATOR

THERMOCOUPLE NUMBER	LOCATION
55	Earth Simulator, Section 1 (Nearest Cooler)
56	Earth Simulator, Section 1 (Nearest Cooler)
57	Earth Simulator, Section 2
58	Earth Simulator, Section 2
59	Earth Simulator, Section 3
60	Earth Simulator, Section 3
61	Earth Simulator, Section 4
62	Earth Simulator, Section 4
63	Earth Simulator, Section 5
64	Earth Simulator, Section 5
65	Earth Simulator, Heater H86-89, Section 1 (Nearest Cooler)
66	Earth Simulator, Heater H86-89, Section 2
67	Earth Simulator, Heater H86-89, Section 3
68	Earth Simulator, Heater H86-89, Section 4
69	Earth Simulator, Heater H85, Section 5

The basic conditions for the four tests are outlined as follows:

Test 1:   Spacecraft temperature = 460°R;
            Earth simulator temperature = 140°R
            (Incident energy flux on cooler opening = 0 Btu/hr-ft^2)

Test 2:   Spacecraft temperature = 460°R;
            Earth simulator temperature = 520°R
            (Incident energy flux on cooler opening = 18.5 Btu/hr-ft^2)

Test 3:   Spacecraft temperature = 460°R
            Earth simulator temperature = 565°R
            (Incident energy flux on cooler opening = 28 Btu/hr-ft^2)

Test 4:   Spacecraft temperature = 500°R;
            Earth simulator temperature = 520°R
            (Incident energy flux on cooler opening = 18.5 Btu/hr-ft^2)

Tests 1, 2, and 3 were used to evaluate the thermal radiative perform-
ance of the shield surfaces; tests 3 and 4 were used to evaluate the
thermal isolation of the shields and radiator from the spacecraft. The
test conditions are summarized in Table 5. Details of the tests are
given in the following paragraphs; test results and an evaluation of cooler
thermal performance are presented in Section VI.

5.3.1   Test 1

Test 1 was performed with the following test conditions: spacecraft skin
temperature (thermocouples 36 to 45) at an average value of 460°R;
earth simulator temperature (thermocouples 55 to 64) at an average
value of 140°R; and chamber wall temperature facing cooler opening at
an average value of 43°R (24°K). No energy was dissipated in the
infrared detector heater during this or subsequent tests, due to a failure
in the heater circuit within the cooler.

During cooldown of the chamber, the temperatures of the primary and
secondary shields (thermocouples 1 to 14) were maintained between 520
and 555°R by use of heaters H90 to H95. Additionally, the temperature
of the earth simulator (thermocouples 55 to 64) was maintained between
520 and 565°R. However, the temperature of the chamber walls facing
the cooler opening did not reach 36°R (20°K) and there was uncertainty
as to the validity of the wall temperatures. After 12 hours of chamber
pumpdown and cooldown, the shield heaters (heaters 90 to 95) were
turned off and, as a checkout of the chamber cooling capacity and earth
simulator heaters, the earth simulator temperature was allowed to
achieve an equilibrium value of 620°R (the temperature of heaters H85
and H86-89 reached an equilibrium value of 660°R). An apparent rise
in the chamber wall temperature was noted.

The earth simulator heaters were shut off and the simulator allowed to
increase to a temperature of 140°R; a corresponding decrease in the
apparent chamber wall temperature was noted. The cooler was allowed

46

TABLE 4

EARTH SIMULATOR HEATERS

HEATER	LOCATION	PURPOSE	THERMOCOUPLE MONITOR	POWER RATING
H85	Earth Simulator Section 5	Control Simulator Temperature	63, 64, 69	120 Volts, 570 Watts
H86-89	Earth Simulator Sections 1,2,3,4	Control Simulator Temperature	55 to 62, 65 to 68	120 Volts, 4400 Watts

TABLE 5

SUMMARY OF TEST CONDITIONS

TEST NO.	CHAMBER WALL TEMPERATURE (°R)	EARTH SIMULATOR TEMPERATURE (°R)	SPACECRAFT SKIN TEMPERATURE (°R)
1	43	140	460
2	61	520	460
3	67	565	460
4	63	520	560

to reach an equilibrium temperature, with the spacecraft skin tempera-ture at 460°R. During cooldown nine of the earth simulator temperature thermocouples became erratic. Following test 1, it was decided to warm up and open the chamber for the following reasons: (1) to determine the reason for the apparent chamber wall temperature increase when the earth simulator temperature was increased (the maximum energy dissipated within the chamber was 1300 watts, whereas the theoretical heat load capacity of the chamber walls in the vicinity of the simulator was 2700 watts); (2) to determine the location of the infrared detector heater cir-cuit opening (the heater circuit opened within the chamber during cool-down of the chamber); and (3) to determine the reason for the erratic readings for nine of the earth simulator temperature thermocouples.

After the chamber was opened, it was noted that at least one chamber temperature sensor on the "West end" door was loose. Reattachments were made and additional redundant sensors were added, especially in the area of the chamber that was viewed by the cooler opening. The circuit opening for the infrared detector heater was somewhere within the cooler package itself. Due to the difficulty in disassembling the package in order to locate the opening, no repairs were made to the cir-cuit. Finally, it was discovered that the erratic simulator temperature readings were due to the unbonding of the simulator heaters from the simulator plane. Therefore, repairs were made to the simulator thermocouples and the heaters were thermally placed in contact with the plane by sandwiching them between the plane and aluminum sheets.

5.3.2   Test 2

Following the repairs made to the chamber temperature sensors and earth simulator, test 2 was started. Test 2 was performed with the following equilibrium test conditions: spacecraft skin temperature at an average value of 460°R; earth simulator temperature at an average value of 520°R; chamber wall temperature facing cooler opening at an average value of 61°R (34°K).

The same procedure was used for control of the shield temperature and earth simulator temperatures during chamber cooldown. The tempera-ture of the earth simulator was limited by two factors: (1) the tempera-ture of the chamber facing the earth simulator increased with an increase in simulator temperature (for example, the temperature of the wall increased from 43°R to 67°R with an increase in the temperature of the simulator from 140°R to 565°R); (2) a large temperature difference developed between the earth simulator plate and simulator heaters, due to the unbonding of the heaters (for example, with the simulator plate at a temperature of 519°R, the temperature of the heaters was 709°R). In order to prevent outgassing, the maximum heater temperature was limited to 780°R. Therefore, the simulator temperature of 620°R which duplicated the heat fluxes for a 200-nmi altitude orbit were not quite duplicated (Figure 23). Thermal equilibrium for the cooler was reached 24 hours after the cooler shield heaters (heaters H90 to H95) were turned off.

48

5.3.3   Test 3

The thermal conditions for test 3 were the same as for test 2 except that the simulator temperature was increased to 565°R, which caused the chamber wall temperature to increase to 37°K. The temperature of the spacecraft skin was maintained at 460°R. At a simulator temperature of 565°R, the average incident heat flux on the cooler is 28 Btu/Hr-ft^2. Thermal equilibrium for test 3 was reached nine hours after the start of the test.

5.3.4   Test 4

The thermal conditions for test 4 were the same as for test 2 except that the spacecraft skin temperature was increased to 560°R. The temperature of the simulator was returned to 520°R, with the chamber wall temperature at 35°K. Thermal equilibrium was reached ten hours after the start of the test.

SECTION VI

TEST RESULTS

The primary objective of the thermal vacuum test program was to verify the thermal design of the model radiative cooler. The goal was to achieve liquid nitrogen temperatures for the first stage of the cooler, on which an infrared detector would be placed. The test results produced higher first stage radiator temperatures than predicted. Depending on the test conditions, the first stage of the cooler reached an equilibrium temperature of 246°R to 200°R. The predicted temperatures for the test conditions were 156°R to 120°R. The test conditions are summarized in Table 5. Based on a correlation of the test and analytical data, the primary reasons for the higher test temperatures were identified as: (1) higher than predicted conductances between the spacecraft structure and the secondary shields, and (2) higher than predicted conductances between stages of the radiator and between the staged radiator base and the spacecraft structure. These differences between the analytical model and test model resulted in higher then predicted secondary shield temperatures and, ultimately, higher than predicted first stage temperatures.

A third reason for the higher than predicted first stage temperatures could be the non-specularity of the shield surfaces, which could cause simulated earth energy to impinge directly on the first stage. For example, as discussed below, the first stage temperature increased from 200°R to 235°R as the energy from the earth simulator incident on the cooler opening increased from 0 Btu/hr-ft^2 to 18.5 Btu/hr-ft^2; however, the staged radiator temperature increased only from 235°R to 236°R as the incident energy increased from 18.5 Btu/hr-ft^2 to 28 Btu/hr-ft^2. Therefore the effect of the non-specularity of the surfaces and its effect on first stage temperatures is more difficult to determine and evaluate. Optical and laser tests prior to testing indicated the acceptability of the shield surfaces. Examination following testing indicated that the surfaces were not visually contaminated.

The cooler and earth simulator temperatures for the four tests are given in Tables 6 through 9 for thermal equilibrium conditions. Also presented in the tables are the analytical model temperature predictions for the corresponding test conditions; the analytical thermal model described in Reference 1 was used for these predictions. The first stage radiator temperatures for the four tests are summarized in Table 10.

The results indicate that the first stage radiator temperatures were 80 to 106R° higher than predicted, depending on the test conditions. By increasing the incident energy flux on the cooler opening from 0 Btu/hr-ft^2 to 18.5 Btu/hr-ft^2 and from 0 Btu/hr-ft to 28 Btu/hr-ft^2 (spacecraft at 460°R), the first stage temperature was increased by 35R° and 36R°, respectively; predictions indicated these temperature increases to be 9R° and 15R°, respectively.

The test results indicate a large change in first stage radiator temperature resulted from increasing the incident heat flux from 0 to 18.5 Btu/hr-ft^2 but a relatively small additional change resulted from increasing the heat flux from 18.5 to 28 Btu/hr-ft^2.

By increasing the temperature of the spacecraft from 460°R to 560°R (incident energy flux on the cooler was 18.5 Btu/hr-ft^2), the test temperature of the first stage increased 10R°. Predictions indicated a temperature rise of 45R°.

The predicted first stage temperatures indicated larger variations due to changes in incident flux and spacecraft temperature than resulted during test. However, the predicted absolute temperatures and radiating ability were lower than the test absolute temperatures and radiating ability. Therefore any small perturbation in the thermal environment would have a greater effect on the lower (predicted) temperatures.

An examination of the test and predicted temperatures presented in Tables 6 through 9 indicates that the closest correspondance between the two temperatures were associated with the primary shield. In fact the test temperatures for the primary shield were generally lower than the predicted temperatures. The largest difference between predicted and test temperatures were associated with the secondary shield, secondary shield insulation, radiator stages, and radiator base. For example, for test 2 conditions, the predicted temperature for the secondary shield was 274°R; the test temperature varied between 386 to 341°R. The predicted temperature for the shield insulation (shield side) was 297°R; the test temperature was 274°R. The predicted radiator base temperature was 292°R; the test temperatures were 348 and 344°R.

Based on the results of the analyses presented in Reference 1, there could be multiple number of reasons for the discrepancy between the predicted and test temperatures, including the following:

(1) Lower than predicted conductance through the secondary shield and primary shield insulation blankets
(2) Heat leaks through the fiberglass structure supporting the shields
(3) Heat leaks through the supports attaching the radiator stages together
(4) Diffuse reflections from the primary shield onto the secondary shield and radiator assembly.
(5) Contamination of the shield surfaces during testing, causing increased shield absorptances and diffuse reflection components
(6) Uncertainties in the temperature of the chamber
(7) Inaccuracy of the thermal analytical model

Due to the multiple modes of heat transfer associated with the radiative cooler, it is different to pinpoint the reason or reasons for the differences between the predicted and test temperatures. However, an examination of the test results and a correlation with the analyses indicates the items 1 through 3 above are primary candidates for the differences between the test

52

TABLE 6

TEST RESULTS - TEST 1

TEST THERMOCOUPLE NUMBER	CORRESPONDING ANALYTICAL NODE NUMBER	THERMOCOUPLE LOCATION	TEST TEMPERATURE (°R)	PREDICTED TEMPERATURE (°R)
1	9	Primary Shield, Center, Top	326	307
2	9	Primary Shield, Center, Bottom	345	307
3	9	Primary Shield, Side, Bottom	321	307
4	7	Primary Shield End 1, Top	350	266
5	7	Primary Shield End 1, Bottom	350	266
6	6	Primary Shield End 2, Top	311	266
7	6	Primary Shield End 2, Bottom	342	266
8	8	Secondary Shield, Center, Bottom	323	270
9	8	Secondary Shield, Center, Top	348	270
10	8	Secondary Shield, Side, Bottom	329	270
11	3	Secondary Shield End 1, Top	355	260
12	3	Secondary Shield End 1, Bottom	366	260
13	4	Secondary Shield End 2, Top	358	260
14	4	Secondary Shield End 2, Bottom	370	260
15	20	Radiator First Stage, Center	201	120
16	20	Radiator First Stage, Center	200	120
17	20	Radiator First Stage, Side	200	120
18	21	Radiator Second Stage, Center	245	145
19	21	Radiator Second Stage, Side	247	145
20	22	Radiator Third Stage, Center	288	187
21	22	Radiator Third Stage, Side	287	187
22	23	Radiator Base, Center	330	289
23	23	Radiator Base, Side	332	289
24	15	Primary Shield Insulation, Shield Side	366	322
25	10	Primary Shield Insulation, Spacecraft Side	438	430
26	17	Primary Shield End 1 Insulation, Shield Side	369	293
27	10	Primary Shield End 1 Insulation, Spacecraft Side	419	430
28	16	Primary Shield End 2 Insulation, Shield Side	372	293
29	10	Primary Shield End 2 Insulation, Spacecraft Side	418	430
30	12	Secondary Shield Insulation, Shield Side	360	294
31	10	Secondary Shield Insulation, Spacecraft Side	432	430
32	13	Secondary Shield End 1 Insulation, Shield Side	390	292
33	10	Secondary Shield End 1 Insulation, Spacecraft Side	418	430
34	14	Secondary Shield End 2 Insulation, Shield Side	419	292
35	10	Secondary Shield End 2 Insulation, Spacecraft Side	---	430
36	--	Spacecraft Back, Top	445	---
37	--	Spacecraft Back, Bottom	450	---
38	--	Spacecraft Left Side, Top	459	---
39	--	Spacecraft Left Side, Bottom	462	---
42	--	Spacecraft Bottom	462	---
43	--	Spacecraft Right Side, Bottom	460	---
44	--	Spacecraft Right Side, Top	462	---
45	--	Spacecraft Top	464	---
46	--	Spacecraft Top, Wing	408	---
47	--	Spacecraft Bottom, Wing	398	---
48	--	Structure Top Base, Center	430	---
49	--	Structure Top Base, Side	426	---

TABLE 6

(CONTINUED)

TEST THERMOCOUPLE NUMBER	CORRESPONDING ANALYTICAL NODE NUMBER	THERMOCOUPLE LOCATION	TEST TEMPERATURE (^{o}R)	PREDICTED TEMPERATURE (^{o}R)
50	---	Structure Bottom Base, Side	432	---
51	---	Structure Bottom Base, Center	434	---
52	---	Fiberglass Structure, Side	426	---
53	---	Fiberglass Structure, Center	432	---
54	---	Fiberglass Structure, Side	429	---
55	---	Earth Simulator, Section 1 (Nearest Cooler)	---	---
56	---	Earth Simulator, Section 1 (Nearest Cooler)	152	---
57	---	Earth Simulator, Section 2	---	---
58	---	Earth Simulator, Section 2	150	---
59	---	Earth Simulator, Section 3	---	---
60	---	Earth Simulator, Section 3	---	---
61	---	Earth Simulator, Section 4	---	---
62	---	Earth Simulator, Section 4	---	---
63	---	Earth Simulator, Section 5	145	---
64	---	Earth Simulator, Section 5	---	---
65	---	Earth Simulator, Heater H89, Section 1	---	---
66	---	Earth Simulator, Heater H88, Section 2	---	---
67	---	Earth Simulator, Heater H87, Section 3	204	---
68	---	Earth Simulator, Heater H86, Section 4	202	---
69	---	Earth Simulator, Heater H85, Section 5	202	---

TABLE 7

TEST RESULTS - TEST 2

TEST THERMOCOUPLE NUMBER	CORRESPONDING ANALYTICAL NODE NUMBER	THERMOCOUPLE LOCATION	TEST TEMPERATURE (°R)	PREDICTED TEMPERATURE (°R)
1	9	Primary Shield, Center, Top	364	395
2	9	Primary Shield, Center, Bottom	392	395
3	9	Primary Shield, Side, Bottom	361	395
4	7	Primary Shield End 1, Top	380	354
5	7	Primary Shield End 1, Bottom	385	354
6	6	Primary Shield End 2, Top	330	354
7	6	Primary Shield End 2, Bottom	373	354
8	8	Secondary Shield, Center, Bottom	341	274
9	8	Secondary Shield, Center, Top	386	274
10	8	Secondary Shield, Side, Bottom	345	274
11	3	Secondary Shield End 1, Top	370	262
12	3	Secondary Shield End 1, Bottom	380	262
13	4	Secondary Shield End 2, Top	375	262
14	4	Secondary Shield End 2, Bottom	383	262
15	20	Radiator First Stage, Center	235	129
16	20	Radiator First Stage, Center	235	129
17	20	Radiator First Stage, Side	262	129
18	21	Radiator Second Stage, Center	263	151
19	21	Radiator Second Stage, Side	303	151
20	22	Radiator Third Stage, Center	303	191
21	22	Radiator Third Stage, Side	344	191
22	23	Radiator Base, Center	348	292
23	23	Radiator Base, Side	386	292
24	15	Primary Shield Insulation, Shield Side	436	397
25	10	Primary Shield Insulation, Spacecraft Side	390	430
26	17	Primary Shield End 1 Insulation, Shield Side	424	361
27	10	Primary Shield End 1 Insulation, Spacecraft Side	391	430
28	16	Primary Shield End 2 Insulation, Shield Side	422	361
29	10	Primary Shield End 2 Insulation, Spacecraft Side	374	430
30	12	Secondary Shield Insulation, Shield Side	434	297
31	10	Secondary Shield Insulation, Spacecraft Side	398	430
32	13	Secondary Shield End 1 Insulation, Shield Side	422	293
33	10	Secondary Shield End 1 Insulation, Spacecraft Side	422	430
34	14	Secondary Shield End 2 Insulation, Shield Side	--	293
35	10	Secondary Shield End 2 Insulation, Spacecraft Side	--	430
36	--	Spacecraft Back, Top	463	---
37	--	Spacecraft Back, Bottom	465	---
38	--	Spacecraft Left Side, Top	460	---
39	--	Spacecraft Left Side, Bottom	458	---
42	--	Spacecraft Bottom	460	---
43	--	Spacecraft Right Side, Bottom	460	---
44	--	Spacecraft Right Side, Top	458	---
45	--	Spacecraft Top	408	---
46	--	Spacecraft Top, Wing	400	---
47	--	Spacecraft Bottom, Wing	432	---
48	--	Structure Top Base, Center	427	---
49	--	Structure Top Base, Side	--	---

TABLE 7

(CONTINUED)

TEST THERMOCOUPLE NUMBER	CORRESPONDING ANALYTICAL NODE NUMBER	THERMOCOUPLE LOCATION	TEST TEMPERATURE (°R)	PREDICTED TEMPERATURE (°R)
50	--	Structure Bottom Base, Side	436	--
51	--	Structure Bottom Base, Center	437	--
52	--	Fiberglass Structure, Side	427	--
53	--	Fiberglass Structure, Center	433	--
54	--	Fiberglass Structure, Side	430	--
55	--	Earth Simulator, Section 1 (Nearest Cooler)	519	--
56	--	Earth Simulator, Section 1 (Nearest Cooler)	518	--
57	--	Earth Simulator, Section 2	528	--
58	--	Earth Simulator, Section 2	522	--
59	--	Earth Simulator, Section 3	521	--
60	--	Earth Simulator, Section 3	533	--
61	--	Earth Simulator, Section 4	517	--
62	--	Earth Simulator, Section 4	513	--
63	--	Earth Simulator, Section 5	529	--
64	--	Earth Simulator, Section 5	524	--
65	--	Earth Simulator, Heater H89, Section 1	709	--
66	--	Earth Simulator, Heater H88, Section 2	655	--
67	--	Earth Simulator, Heater H87, Section 3	692	--
68	--	Earth Simulator, Heater H86, Section 4	697	--
69	--	Earth Simulator, Heater H85, Section 5	716	--

TABLE 8

TEST RESULTS - TEST 3

TEST THERMOCOUPLE NUMBER	CORRESPONDING ANALYTICAL NODE NUMBER	THERMOCOUPLE LOCATION	TEST TEMPERATURE (°R)	PREDICTED TEMPERATURE (°R)
1	9	Primary Shield, Center, Top	361	320
2	9	Primary Shield, Center, Bottom	372	320
3	9	Primary Shield, Side, Bottom	361	320
4	7	Primary Shield End 1, Top	379	378
5	7	Primary Shield End 1, Bottom	388	378
6	6	Primary Shield End 2, Top	320	378
7	6	Primary Shield End 2, Bottom	372	378
8	8	Secondary Shield, Center, Bottom	332	276
9	8	Secondary Shield, Center, Top	388	276
10	8	Secondary Shield, Side, Bottom	335	276
11	3	Secondary Shield End 1, Top	363	263
12	3	Secondary Shield End 1, Bottom	374	263
13	4	Secondary Shield End 2, Top	367	263
14	4	Secondary Shield End 2, Bottom	378	263
15	20	Radiator First Stage, Center	234	135
16	20	Radiator First Stage, Center	236	135
17	20	Radiator First Stage, Side	236	135
18	21	Radiator Second Stage, Center	260	156
19	21	Radiator Second Stage, Side	261	156
20	22	Radiator Third Stage, Center	300	192
21	22	Radiator Third Stage, Side	298	192
22	23	Radiator Base, Center	338	293
23	23	Radiator Base, Side	342	293
24	15	Primary Shield Insulation, Shield Side	382	421
25	10	Primary Shield Insulation, Spacecraft Side	436	430
26	17	Primary Shield End 1 Insulation, Shield Side	386	382
27	10	Primary Shield End 1 Insulation, Spacecraft Side	424	430
28	16	Primary Shield End 2 Insulation, Shield Side	388	382
29	10	Primary Shield End 2 Insulation, Spacecraft Side	424	430
30	12	Secondary Shield Insulation, Shield Side	362	298
31	10	Secondary Shield Insulation, Spacecraft Side	432	430
32	13	Secondary Shield End 1 Insulation, Shield Side	394	293
33	10	Secondary Shield End 1 Insulation, Spacecraft Side	420	430
34	14	Secondary Shield End 2 Insulation, Shield Side	423	293
35	10	Secondary Shield End 2 Insulation, Spacecraft Side	---	430
36	--	Spacecraft Back, Top	462	---
37	--	Spacecraft Back, Bottom	468	---
38	--	Spacecraft Left Side, Top	460	---
39	--	Spacecraft Left Side, Bottom	460	---
42	--	Spacecraft Bottom	462	---
43	--	Spacecraft Right Side, Bottom	460	---
44	--	Spacecraft Right Side, Top	463	---
45	--	Spacecraft Top	463	---
46	--	Spacecraft Top, Wing	410	---
47	--	Spacecraft Bottom, Wing	402	---
48	--	Structure Top Base, Center	430	---
49	--	Structure Top Base, Side	426	---

TABLE 8

(CONTINUED)

TEST THERMOCOUPLE NUMBER	CORRESPONDING ANALYTICAL NODE NUMBER	THERMOCOUPLE LOCATION	TEST TEMPERATURE (°R)	PREDICTED TEMPERATURE (°R)
50	--	Structure Bottom Base, Side	434	---
51	--	Structure Bottom Base, Center	434	---
52	--	Fiberglass Structure, Side	428	---
53	--	Fiberglass Structure, Center	434	---
54	--	Fiberglass Structure, Side	430	---
55	--	Earth Simulator, Section 1 (Nearest Cooler)	565	---
56	--	Earth Simulator, Section 1 (Nearest Cooler)	562	---
57	--	Earth Simulator, Section 2	574	---
58	--	Earth Simulator, Section 2	564	---
59	--	Earth Simulator, Section 3	564	---
60	--	Earth Simulator, Section 3	575	---
61	--	Earth Simulator, Section 4	560	---
62	--	Earth Simulator, Section 4	556	---
63	--	Earth Simulator, Section 5	574	---
64	--	Earth Simulator, Section 5	771	---
65	--	Earth Simulator, Heater H89, Section 1	787	---
66	--	Earth Simulator, Heater H88, Section 2	703	---
67	--	Earth Simulator, Heater H87, Section 3	773	---
68	--	Earth Simulator, Heater H86, Section 4	776	---
69	--	Earth Simulator, Heater H85, Section 5	775	---

TABLE 9

TEST RESULTS - TEST 4

TEST THERMOCOUPLE NUMBER	CORRESPONDING ANALYTICAL NODE NUMBER	THERMOCOUPLE LOCATION	TEST TEMPERATURE (°R)	PREDICTED TEMPERATURE (°R)
1	9	Primary Shield, Center, Top	384	413
2	9	Primary Shield, Center, Bottom	418	413
3	9	Primary Shield, Side, Bottom	380	413
4	7	Primary Shield End 1, Top	416	367
5	7	Primary Shield End 1, Bottom	424	367
6	6	Primary Shield End 2, Top	342	367
7	6	Primary Shield End 2, Bottom	407	367
8	8	Secondary Shield, Center, Bottom	363	300
9	8	Secondary Shield, Center, Top	420	300
10	8	Secondary Shield, Side, Bottom	370	300
11	3	Secondary Shield End 1, Top	414	285
12	3	Secondary Shield End 1, Bottom	429	285
13	4	Secondary Shield End 2, Top	420	285
14	4	Secondary Shield End 2, Bottom	435	285
15	20	Radiator First Stage, Center	246	156
16	20	Radiator First Stage, Center	246	156
17	20	Radiator First Stage, Side	246	156
18	21	Radiator Second Stage, Center	282	196
19	21	Radiator Second Stage, Side	284	196
20	22	Radiator Third Stage, Center	331	230
21	22	Radiator Third Stage, Side	329	230
22	23	Radiator Base, Center	384	327
23	23	Radiator Base, Side	386	327
24	15	Primary Shield Insulation, Shield Side	428	419
25	10	Primary Shield Insulation, Spacecraft Side	526	510
26	17	Primary Shield End 1 Insulation, Shield Side	436	397
27	10	Primary Shield End 1 Insulation, Spacecraft Side	504	510
28	16	Primary Shield End 2 Insulation, Shield Side	440	397
29	10	Primary Shield End 2 Insulation, Spacecraft Side	503	510
30	12	Secondary Shield Insulation, Shield Side	415	368
31	10	Secondary Shield Insulation, Spacecraft Side	522	510
32	13	Secondary Shield End 1 Insulation, Shield Side	458	364
33	10	Secondary Shield End 1 Insulation, Spacecraft Side	501	510
34	14	Secondary Shield End 2 Insulation, Shield Side	505	364
35	10	Secondary Shield End 2 Insulation, Spacecraft Side	---	510
36	--	Spacecraft Back, Top	568	---
37	--	Spacecraft Back, Bottom	569	---
38	--	Spacecraft Left Side, Top	560	---
39	--	Spacecraft Left Side, Bottom	558	---
42	--	Spacecraft Bottom	560	---
43	--	Spacecraft Right Side, Bottom	560	---
44	--	Spacecraft Right Side, Top	556	---
45	--	Spacecraft Top	---	---
46	--	Spacecraft Top, Wing	474	---
47	--	Spacecraft Bottom, Wing	465	---
48	--	Structure Top Base, Center	516	---
49	--	Structure Top Base, Side	510	---

TABLE 9

(CONTINUED)

TEST THERMOCOUPLE NUMBER	CORRESPONDING ANALYTICAL NODE NUMBER	THERMOCOUPLE LOCATION	TEST TEMPERATURE ($^\circ$R)	PREDICTED TEMPERATURE ($^\circ$R)
50	--	Structure Bottom Base, Side	523	--
51	--	Structure Bottom Base, Center	525	--
52	--	Fiberglass Structure, Side	510	--
53	--	Fiberglass Structure, Center	522	--
54	--	Fiberglass Structure, Side	512	--
55	--	Earth Simulator, Section 1 (Nearest Cooler)	520	--
56	--	Earth Simulator, Section 1 (Nearest Cooler)	520	--
57	--	Earth Simulator, Section 2	529	--
58	--	Earth Simulator, Section 2	520	--
59	--	Earth Simulator, Section 3	522	--
60	--	Earth Simulator, Section 3	520	--
61	--	Earth Simulator, Section 4	515	--
62	--	Earth Simulator, Section 4	514	--
63	--	Earth Simulator, Section 5	528	--
64	--	Earth Simulator, Section 5	523	--
65	--	Earth Simulator, Heater HB9, Section 1	722	--
66	--	Earth Simulator, Heater HB8, Section 2	649	--
67	--	Earth Simulator, Heater HB7, Section 3	706	--
68	--	Earth Simulator, Heater HB6, Section 4	715	--
69	--	Earth Simulator, Heater HB5, Section 5	712	--

TABLE 10

SUMMARY OF FIRST STAGE TEST AND ANALYTICAL TEMPERATURES

TEST	TEST CONDITIONS	FIRST STAGE TEMPERATURES (°R)	
		TEST	PREDICTED
1	• Spacecraft Temperature = 460°R • Earth Simulator Temperature = 140°R (incident energy flux on cooler opening = 0 Btu/hr-ft^2)	200	120
2	• Spacecraft Temperature = 460°R • Earth Simulator Temperature = 520°R (incident energy flux on cooler opening = 13.5 Btu/hr-ft^2)	235	129
3	• Spacecraft Temperature = 460°R • Earth Simulator Temperature = 565°R (incident energy flux on cooler opening = 28 Btu/hr-ft^2)	236	135
4	• Spacecraft Temperature = 560°R • Earth Simulator Temperature = 520°R (incident energy flux on cooler opening = 18.5 Btu/hr-ft^2)	246	156

and analysis results, although diffusely reflected energy off the shields and onto the radiator stage would cause a temperature rise in the radiator, as shown in Figure 48 of Reference 1. A discussion of the correlation between test and analytical results follows.

Based on the results of the analyses presented in Reference 1, the temperature of the primary shield, which is higher than the temperature of the secondary shield, is dependent on absorbed fluxes from the earth simulator and, to a lesser extent, thermal isolation from the complete system. However, the temperature of the secondary shield is heavily dependent on thermal isolation from the spacecraft, the temperature of the secondary shields, and the ability of the shields to reflect specularly.

The laser tests and optical tests performed at Philco-Ford (Paragraph 3.4) indicated that the parabola shields performed optically as required. A visual examination of the shields indicated no contamination of the surfaces, although no optical or laser tests were performed on the surfaces following testing.

From the results of test 1, with no energy flux incident on the cooler opening, the first stage temperature was 80R° higher than predicted. However, a better correlation between predicted and test temperatures was achieved by degrading the performance of the secondary shield insulation, by increasing the conductance between the secondary shield and structure via the fiberglass supports, and by increasing the conductance between the radiator stages. The results of the correlation are given in Table 11. For this correlation, the radiator base temperature used in the predictions was fixed at the test temperature. Additionally, the conductance between stages of the radiator was increased by a factor of five, and the conductance in the secondary shield insulation was increased by a factor of four.

The temperature of the first stage of the radiator increased from 200°R to 236°R as the incident heat flux on the cooler opening was increased from 0 to 28 Btu/hr-ft². The correlation of the test and analysis temperatures for these conditions is more difficult to determine. As indicated above, the pretest and post-test condition of the shields appeared to be acceptable.

The predicted temperatures assumed isothermal nodes for the shield parabolas and each of the shield ends. However, the test results indicated that the shields were not isothermal, as indicated in Tables 6 to 9. For example, in test 3 (Table 8) the temperature of the primary parabola shield at the shield top (furthest from the radiator) was 361°R (thermocouple 1), whereas the temperature at the bottom of the shield (nearest the radiator) was 392°R at the center and 361°R at the side. Similar temperature distributions occurred for the other shields. The differences in temperatures can be attributed to the following: low lateral thermal conductance in the shield surfaces (aluminized mylar); uneven incident heat flux at the cooler opening (Figure 24); and localized thermal heat leaks to and from the spacecraft along the shield surfaces.

TABLE 11

CORRELATION OF ANALYTICAL AND TEST RESULTS – TEST 1

TEST THERMOCOUPLE NUMBER	CORRESPONDING ANALYTICAL NODE NUMBER	THERMOCOUPLE LOCATION	TEST TEMPERATURE (°R)	PREDICTED TEMPERATURE (°R)
1	9	Primary Shield, Center, Top	326	373
2	9	Primary Shield, Center, Bottom	345	373
3	9	Primary Shield, Side, Bottom	321	373
4	7	Primary Shield End 1, Top	350	383
5	7	Primary Shield End 1, Bottom	350	383
6	6	Primary Shield End 2, Top	311	383
7	6	Primary Shield End 2, Bottom	342	383
8	8	Secondary Shield, Center, Bottom	323	358
9	8	Secondary Shield, Center, Top	348	358
10	8	Secondary Shield, Side, Bottom	329	358
11	3	Secondary Shield End 1, Top	355	369
12	3	Secondary Shield End 1, Bottom	366	369
13	4	Secondary Shield End 2, Top	358	369
14	4	Secondary Shield End 2, Bottom	370	369
15	20	Radiator First Stage, Center	201	189
16	20	Radiator First Stage, Center	200	189
17	20	Radiator First Stage, Side	200	189
18	21	Radiator Second Stage, Center	245	236
19	21	Radiator Second Stage, Side	247	236
20	22	Radiator Third Stage, Center	288	303
21	22	Radiator Third Stage, Side	287	303
22	23	Radiator Base, Center	330	331
23	23	Radiator Base, Side	332	331
24	15	Primary Shield Insulation, Shield Side	366	377
25	10	Primary Shield Insulation, Spacecraft Side	438	430
26	17	Primary Shield End 1 Insulation, Shield Side	369	387
27	10	Primary Shield End 1 Insulation, Spacecraft Side	419	430
28	16	Primary Shield End 2 Insulation, Shield Side	372	378
29	10	Primary Shield End 2 Insulation, Spacecraft Side	418	430
30	12	Secondary Shield Insulation, Shield Side	360	361
31	10	Secondary Shield Insulation, Spacecraft Side	432	430
32	13	Secondary Shield End 1 Insulation, Shield Side	390	380
33	10	Secondary Shield End 1 Insulation, Spacecraft Side	418	430
34	14	Secondary Shield End 2 Insulation, Shield Side	419	384
35	10	Secondary Shield End 2 Insulation, Spacecraft Side	---	430
36	--	Spacecraft Back, Top	475	---
37	--	Spacecraft Back, Bottom	470	---
38	--	Spacecraft Left Side, Top	461	---
39	--	Spacecraft Left Side, Bottom	462	---
42	--	Spacecraft Bottom	462	---
43	--	Spacecraft Right Side, Bottom	460	---
44	--	Spacecraft Right Side, Top	462	---
45	--	Spacecraft Top	464	---
46	--	Spacecraft Top, Wing	408	---
47	--	Spacecraft Bottom, Wing	398	---
48	--	Structure Top Base, Center	430	---
49	--	Structure Top Base, Side	426	---

TABLE 11

(CONTINUED)

TEST THERMOCOUPLE NUMBER	CORRESPONDING ANALYTICAL NODE NUMBER	THERMOCOUPLE LOCATION	TEST TEMPERATURE (°R)	PREDICTED TEMPERATURE (°R)
50	---	Structure Bottom Base, Side	432	---
51	---	Structure Bottom Base, Center	434	---
52	---	Fiberglass Structure, Side	426	---
53	---	Fiberglass Structure, Center	432	---
54	---	Fiberglass Structure, Side	429	---
55	---	Earth Simulator, Section 1 (Nearest Cooler)	---	---
56	---	Earth Simulator, Section 1 (Nearest Cooler)	152	---
57	---	Earth Simulator, Section 2	---	---
58	---	Earth Simulator, Section 2	150	---
59	---	Earth Simulator, Section 3	---	---
60	---	Earth Simulator, Section 3	---	---
61	---	Earth Simulator, Section 4	---	---
62	---	Earth Simulator, Section 4	---	---
63	---	Earth Simulator, Section 5	145	---
64	---	Earth Simulator, Section 5	---	---
65	---	Earth Simulator, Heater H89, Section 1	---	---
66	---	Earth Simulator, Heater H88, Section 2	---	---
67	---	Earth Simulator, Heater H87, Section 3	204	---
68	---	Earth Simulator, Heater H86, Section 4	202	---
69	---	Earth Simulator, Heater H85, Section 5	202	---

SECTION VII

CONCLUSIONS

Based on the results of an earlier study performed by Philco-Ford for Wright-Patterson Air Force Base, an infrared detector radiative cooler designed for use in a 200 nautical mile altitude orbit was fabricated, assembled, and tested in a 36°R thermal vacuum environment. Thermal isolation of the infrared detector radiator was achieved by use of a staged radiator assembly. Rejection of incident earth energy was achieved by use of two high reflectance, specular staged shields. Fabrication techniques were developed for the cooler. A unique method of achieving shield surfaces, which met the thermal and optical requirements for the cooler, was used. The method consisted essentially of the bonding of a high reflectance specular, aluminized-mylar shield surface to parabolic and flat honeycomb substrates.

A method was developed for the simulation of earth energy incident on the cooler opening. The earth energy simulation was achieved by use of a flat 4-ft by 4-ft plate, painted black, and placed in the relative position of the earth in front of the cooler opening. The temperature of the plate was regulated to duplicate earth albedo and emission energies by use of heaters attached to the opposite side of the plate.

A total of four tests were performed in the AEDC 7V, 36°R thermal vacuum chamber. The tests produced higher than predicted temperatures for the radiator. The first stage of the radiator reached a maximum equilibrium temperature of 236°R with the simulator at a temperature of 565°R and the spacecraft skin at a temperature of 560°R; the predicted radiator temperature for this condition was 156°R. The radiator reached a minimum equilibrium temperature of 200°R with the simulator at a temperature of 140°R and the spacecraft skin at a temperature of 460°R; the predicted radiator temperature for this test condition was 120°R. Based on a correlation of the test and analytical data, the primary reasons for the higher test temperatures were identified as (1) higher than predicted thermal conductances between the spacecraft structure and the secondary shield assembly, and (2) higher than predicted thermal conductances between stages of the radiator base and the spacecraft structure.

SECTION VIII

REFERENCES

1. C. A. Zierman, R. H. Hulett, W. F. Schmidt, and R. A. Wiedeman, "Feasibility Study and Development Design of a Passive Radiative Cooler for Infrared Detectors," AFFDL-TR-69-122, December 1969

2. R. E. Rolling and C. L. Tien, "Total Specular Reflectance of Rough Metallic Surfaces," Journal of Spacecraft and Rockets, December 1966, pp. 1719-1722

3. "Test Plan - Fabrication and Instrumentation of an Experimental Passive Radiative Infrared Detector Cooler for Spacecraft Applications," dated 30 April 1971

DOCUMENT CONTROL DATA - R & D

(Security classification of title, body of abstract and indexing annotation must be entered when the overall report is classified)

1. ORIGINATING ACTIVITY (Corporate author)	2a. REPORT SECURITY CLASSIFICATION
Western Development Laboratories Division Philco-Ford Corporation Palo Alto, California	Unclassified
	2b. GROUP None

3. REPORT TITLE

Fabrication and Instrumentation of an Experimental Passive Radiative Infrared Detector for Spacecraft Applications

4. DESCRIPTIVE NOTES (Type of report and inclusive dates)

5. AUTHOR(S) (First name, middle initial, last name)

Werner F. Schmidt
Harold L. Hillesland
Carl A. Zierman

6. REPORT DATE	7a. TOTAL NO. OF PAGES	7b. NO. OF REFS
1971	78	3

8a. CONTRACT OR GRANT NO. F33615-71-C-1025	9a. ORIGINATOR'S REPORT NUMBER(S)
b. PROJECT NO. 1470	
c.	9b. OTHER REPORT NO(S) (Any other numbers that may be assigned this report)
d.	AFFDL-TR-71-125

10. DISTRIBUTION STATEMENT

This document is subject to special export controls and each transmittal to foreign governments or foreign nations may be made only with prior approval of AFFDL (FEE) Wright-Patterson Air Force Base, Ohio 45433.

11. SUPPLEMENTARY NOTES	12. SPONSORING MILITARY ACTIVITY Air Force Flight Dynamics Laboratories Wright-Patterson Air Force Base Ohio 45433

13. ABSTRACT

A thermal experimental model of a passive radiative cooler for use on an earth orbiting spacecraft was fabricated, assembled, and tested in a thermal vacuum environment. The design of the cooler was based on the results of a previous thermal analysis and design study performed by Philco-Ford for Wright-Patterson Air Force Base. The cooler was assumed to be used on a spacecraft in a 200 nautical mile altitude earth orbit in the plane of the ecliptic. The objective of the program was to verify the thermal performance of the cooler. Thermal analysis predicted an orbital temperature of 146°R for the radiator of the cooler. The tests produced higher than predicted temperatures for the radiator. Depending on the test conditions, a temperature of 246°R to 200°R was achieved for the radiator. The primary reasons for the higher than predicted temperatures were identified as higher than predicted thermal conductances between the simulated spacecraft and the cooler shield and radiator surfaces.

DD FORM **1473** REPLACES DD FORM 1473, 1 JAN 64, WHICH IS
1 NOV 65 OBSOLETE FOR ARMY USE.

14. KEY WORDS	LINK A		LINK B		LINK C	
	ROLE	WT	ROLE	WT	ROLE	WT
Radiative Cooler						
Infrared Detectors						
Passive Thermal Control						
Cryogenic						
Spacecraft						
Thermal Vacuum Testing						